Mechanisms and scenarios of the unprecedent flooding event in South Brazil 2024

Leonardo Laipelt[1], Fernando Mainardi Fan[1], Rodrigo Cauduro Dias de Paiva[1], Matheus Sampaio[1], Walter Collischonn[1] and Anderson Ruhoff[1]

[1]Institute of Hydraulic Research (IPH), Federal University of Rio Grande do Sul, Porto Alegre, Brazil

Correspondence to: Leonardo Laipelt (leonardo.laipelt@ufrgs.br)

Abstract. In May 2024, an extraordinary precipitation event ~~in southern Brazil~~ triggered record floods in ~~South~~ southern Brazil, ~~specially~~ particularly ~~over a~~impacting complex river-estuary-lagoon systems~~ system that includes rivers as Jacuí and Taquari, draining into Guaíba and Patos Lagoon~~, and resulting in~~. It resulted in~~ unprecedented impacts on the local population and infrastructure. ~~Considering~~ As climate change projections indicate an increase in such events for the region~~past observations and projections indicating an increase in flood events in the region due to climate change~~, understanding these flooding processes i~~in the region i~~s essential for better preparing cities for future events like the May 2024 flood. In this context, hydrodynamic modelling ~~serves~~ is~~as~~ an important tool for reproducing and analysing this past extreme event. This paper presents the first detailed hydrodynamic assessment of this unprecedented flood, the worst registered natural disaster in Brazilian history. We also performed the first validation of a detailed hydrodynamic model using new observations from the SWOT satellite. The study investigates the main mechanisms that governed the disaster and assesses scenarios for hydraulic flood control interventions currently under public debate, with a ~~This study aims to assess the detailed hydrodynamic mechanisms and processes that occurred during this historical flood event and scenarios of direct interventions for flood control that came into the public debate after the event. The focus is~~focus on the most populated areas ~~at~~ of the Metropolitan region of Porto Alegre (RMPA) capital city. ~~We calibrate and validate a two-dimensional hydrodynamic model to precisely replicate the May 2024 flood .~~ The results demonstrated that the model accurately ~~represents~~ represented the event, with average NSE, RMSE and BIAS of 0.82, 0.71 meters and -0.47 meters, respectively, across the ~~main rivers in the basin~~basin's main rivers. Furthermore, the ~~flood extent simulation~~simulated flood extent ~~represented~~ showed an 83% agreement ~~of the affected area, as compared to~~with high-resolution satellite images. Our analysis of the governing mechanisms ~~that influenced the event~~ showed that the Taquari River was ~~the main~~mainly responsible for the peak in the RMPA, while the Jacuí River contributed ~~the~~ most to the ~~duration of the flood~~flood's duration. Additionally, the synchronization of the flood peaks from both rivers could have increased water levels by 0.82 meters. Evaluated hydraulic interventions ~~for flood mitigation~~ demonstrated that the effectiveness of the proposed measures varied by location, with ~~usually low~~a generally limited influence ~~in the~~on RMPA water levels (lower than 0.38 m). By accurately assessing the May 2024 flood, this study enhances the understanding of a complex river-estuary-lagoon system, quantifies the impacts of adverse scenarios, and reveals the limitations of potential hydraulic

structure interventions. Finally, modelling this unprecedented event offers valuable insights for future research and global flood management policies.~~Major lessons related to the behaviour of river lagoon hydrodynamic systems and to the relevance of structural measures for such cases are discussed, which are of broader interest for future research and decision making around the globe.~~

1. Introduction

The May 2024 flood ~~that occurred in South~~in southern Brazil ~~can be~~is considered the worst natural disaster in Brazilian history given its magnitude, spatial coverage and impacts (Collischonn et al., 2025). ~~(Collischonn et al., 2025).~~ The flood affected hundreds of thousands of people, displacing entire ~~neighborhoods~~neighbourhoods, causing numerous fatalities, ~~causing~~ and inflicting widespread damage ~~to~~ on urban infrastructure and agricultural lands.~~lands, while also leading in numerous fatalities. Floods becomes a major concern and one of the most relevant disasters in terms of impacts, with the potential to disrupts societies on a unprecedent scale. The rising frequency and severity of flood events are closely linked to ongoing climate change, as global temperatures increase due to global warming , affecting the hydrological cycle and leading to more intense and frequent rainfall events . However, the relationship between climate change and flood is complex, with impacts vary regionally and influenced by multiple factors .~~

Floods in southern Brazil, situated in the sub-tropical and temperate portions of South America, have increased significantly in recent decades, a trend that has been supported by both historical data and climate projections (Ávila et al., 2016; Bartiko et al., 2019; Brêda et al., 2023; Chagas et al., 2022). Nationally, flood generation in Brazil is driven by a variety of mechanisms. These include intense convective storms causing urban flash floods (Cavalcante et al., 2020; Lima and Barbosa, 2019; Marengo et al., 2023), persistent rainfall associated with South Atlantic Convergence Zone (SACZ) leading to large-scale riverine floods, and the influence of major teleconnections like the El Niño-Southern Oscillation (ENSO). Specifically, in the southern region, the primary drivers are often intense frontal systems that bring widespread and prolonged precipitation (Ávila et al., 2016; Damião Mendes and Cavalcanti, 2014). Moreover, climate change is intensifying this scenario by increasing hydroclimate and hydrological volatility and altering flood-generating mechanisms (Hammond et al., 2025; Stevenson et al., 2022; Swain et al., 2025). This, in turn, increases the frequency and severity of floods, particularly through compound events (Heinrich et al., 2023; Hendry et al., 2019; Leonard et al., 2014).

The ~~Floods in southern Brazil, situated at the sub-tropical and temperate portions of South America, have increase significant in recent decades, which has been supported by both historical data and climate projections . These studies suggested an increase in heavy rainfall events and maximum discharge in the region due to climate change, but also attributing to changes of the El Niño-Southern Oscillation (ENSO) and in the South American Convergence Zone (SACZ). In instance, Chagas et al. (2022) analysed streamflow data across South America and showed that flooding in Southern Brazil is on the rise and indicating~~

~~a possible link with ENSO variations. Breda et al. (2023) demonstrated that different climate models, based on CMIP5 scenarios, predict a continued increase in flood frequency due to heightened extreme precipitation events in the region. The same southern regions of Brazil experienced catastrophic flooding in May 2024, triggered by extreme rainfall that surpassed previous water level record.~~

~~The major impacted areas in southern Brazil during the~~ May 2024 floods ~~are~~in southern Brazil primarily impacted the state ~~situated in the~~of Rio Grande do Sul State (RS), ~~including~~ including ~~the~~ its capital, ~~city~~ Porto Alegre. ~~Rainfall~~ ~~O~~observed rainfall data indicated ~~that~~ precipitation ~~has~~ exceeded 500 ~~millimeters~~millimetres within a two-day period, ~~with~~ while some locations accumulate~~ding~~ up to 900 ~~millimeters~~millimetres ~~in~~ over 35 days (Collischonn et al., 2024). Therefore~~As consequence~~, flood ~~has achieved~~reached ~~breaking record~~record-breaking levels in ~~many~~ numerous cities ~~in~~ within the Patos Lagoon basin, which ~~covered~~ covers half of ~~Rio Grande do Sul~~the state.

Several impacts ~~in~~ on the population and ~~cities~~ urban infrastructure were ~~observed~~ concentrated in the Metropolitan Region of Porto Alegre (RMPA), ~~where nearly 40% of the state's population (over 4 million people) resides~~home to over 4 million people (nearly 40% of the state's population). According to official government surveys, approximately 300,000 people in RMPA were directly affected by ~~the flood in the RMPA~~the flooding.~~,~~ ~~with the situation worsened~~The situation was significantly exacerbated by the failure of local flood protection systems. Given these devasting impacts, there is a critical need to employ advanced assessment~~s~~ tools, such as hydrodynamic ~~modeling~~modelling, to better understand and manage such extreme events.~~.~~ ~~A complete comprehensive hydrological description the disaster is given by Collischonn et al. .~~

The Patos Lagoon basin, ~~where the main~~most severely impacted by the May 2024 disaster ~~occurred~~, is a unique ~~single~~ natural system ~~in the world~~. Its complex ~~The~~ watershed ~~is constituted by a combination of fast~~combines fast-flowing mountainous rivers ~~and one large~~with a large, slow floodplain river~~s~~. ~~. These tributaries converge into~~~~downstream, all flowing to~~ a relatively short, wide body ~~and wide river~~ named Guaíba River (which is also called a lake due to its physical characteristics).~~,~~ The Guaíba, in turn, flows into~~and downstream the Guaíba inflows to~~ the Patos Lagoon itself, ~~which is~~ an extensive water body known ~~and~~ as the ~~greatest~~ world's largest choked lagoon ~~in the world~~ (Kjerfve, 1986).

After the disaster, many questions were raised regarding the function of the natural system: the relevance of the upstream rivers, the slopes generated by water inflows and even ~~if extra~~whether extra outlets ~~in the~~from the lagoon to the sea ~~would not have~~ might have avoided the flooding in~~at~~ upstream areas (Hunt et al., 2024; Silva et al., 2024a). From our understanding, the tool to answer some of those questions is a hydrodynamic model capable of properly representing the system. ~~, that must~~This model must be properly validated using not only gauge observations but also state-of-the-art remote sensing data.

Hydrodynamic modelling has been widely used for flood assessment, including models such as HEC-RAS (USACE, 2016), LISFLOOD-FP (Bates and De Roo, 2000) and Delft3D (Lesser et al., 2004). These ~~are~~ physically-based models ~~to~~ represent water flow across natural systems, ~~providing~~ accurately ~~accurate flood~~ predicting flood propagation and extent (Ming et al., 2020; Paiva et al., 2013; Timbadiya et al., 2015). Their ~~Additionally, they have the~~ ability to reproduce floods in~~with~~ high-resolution ~~details, enabling the reconstruction of~~makes them ideal for reconstructing past events and simulation ~~record-breaking events and the simulation of~~ various scenarios (Bates et al., 2003; Fewtrell et al., 2011; Marks and Bates, 2000). For

Formatted: Font color: Auto

instance, these models are particularly useful for studying complex interactions in medium-to-large basins (O'Loughlin et al., 2020; Paiva et al., 2013), where precipitation is expected to become more concentrated. In these coupled systems, the synchrony between the peak flows of major tributaries and the estuary–lagoon water level is a primary determinant of flood severity, directly informing the timing and feasibility of structural and operational measures (Guse et al., 2020). While previous studies have often focused on individual rivers or local interventions (Dutta et al., 2007; Patel et al., 2017; Timbadiya et al., 2015; Zarzuelo et al., 2015), few have examined synchrony and mitigation within an integrated, river–estuary–lagoon framework at regional scale. Moreover, simulating flood mitigation scenarios is essential for evaluating interventions, defining optimal locations for new structures, assessing the efficiency of existing ones (Abdella and Mekuanent, 2021; Ghanbarpour et al., 2013; Zhang et al., 2021), and identifying areas of high risk (Cai et al., 2019; Li et al., 2019; Masood and Takeuchi, 2012). Among different applications, Neal et al. (2011) assessed the 2007 United Kingdom~~ton~~ floods using the LISFLOOD-FP two-dimensional model to simulate water levels in urban areas, validating flood extent with satellite imagery. Marengo et al. (2023) utilized the HEC-RAS 2D model to examine flood inundation extent resulting from an extreme precipitation event in Recife, Northeast Brazil. In southern Brazil, there are few studies using hydrodynamic models to evaluate historical water levels in the Patos Lagoon basin (Alves et al., 2022; Fernandes et al., 2001, 2002; Möller et al., 1996). Alves et al. (2022) evaluated the ability of large-scale models to generate flood maps, comparing results with satellite imagery and flood extent from 2D hydrodynamic flood simulations. Fernandes et al. (2001) calibrated and validated the TELEMAC-2D model to simulate water levels over the Patos Lagoon, finding good agreement with observational data.

This study develops the first detailed hydrodynamic assessment of the unprecedented flood that occurred in 2024 in south Brazil, which represents the worst disaster in Brazilian history. In addition to this novelty, it is the first study to utilize SWOT satellite altimetry data for model evaluation. Our primary goals are to investigate the main mechanisms governing this flood disaster and to assess hydraulic intervention scenarios for flood control in the region, which are currently under public debate. To achieve this, we address urgent and unresolved questions raised by the May-2024 flood regarding: (a) the relative influence of tributary inflows on RMPA water levels and inundation, (b) the consequences of potential peak synchrony between the main rivers, and (c) whether additional lagoon–ocean outlets or channel operations would have mitigated upstream flooding. Prior studies did not jointly address these system-scale dynamics due to limited integrated datasets and validation across the river–estuary–lagoon continuum. Leveraging detailed bathymetry, ADCP transects, continuous gauges, satellite flood extent, and SWOT altimetry (Biancamaria et al., 2016; Fu et al., 2024), we develop and validate a 2D hydrodynamic model to quantify mechanisms and test counterfactual scenarios. This design yields decision-relevant evidence for stakeholders and government agencies seeking to enhance protection in the most affected areas, and ultimately allows comprehension of how this unique natural system works under extreme conditions. The insights from this study are therefore highly relevant for other complex, large-scale hydrodynamic coastal and deltaic regions.

~~This study aims to enhance our understanding of flooding mechanisms in South Brazil, using the May 2024 flood as a reference, with focus on the RMPA region. Beyond being the first detailed hydrodynamic assessment of this~~

Formatted: Font color: Auto
Formatted: Font color: Auto
Formatted: Font color: Auto
Formatted: Font color: Auto
Formatted: Font color: Auto
Formatted: Font color: Auto
Formatted: Font color: Auto
Formatted: English (United States)
Formatted: Font color: Auto
Formatted: Font color: Auto
Formatted: Font color: Auto

~~unprecedented event at this singular environment, the present research is of broad interest due to other several reasons: a benchmark is set in terms of flood modelling validation using a two-dimensional hydrodynamic model and multiple data sources for RMPA; for the first time on authors knowledge altimetry information from SWOT mission is used to validate the modelling of such an extreme event; the contribution of each river was evaluated, as well as an assessment of a river peak synchronization scenario that could have worsened the event; the relevance of structural solutions for extreme floodings for environments controlled by both upstream and downstream characteristics is discussed; lessons and examples that can be used by decision makers from other locations with similar issues around the globe are discussed.~~

2. Study Area

Formatted: Space After: 0 pt

~~Study Area~~

The Patos Lagoon basin encompasses 182,000 km² (**Figure 1a**), with its headwaters situated in Rio Grande do Sul's north-central region, characterized by deep canyon valleys transitioning into vast lowlands. The primary upstream tributaries, the Taquari, Jacuí, Caí, Sinos and Gravataí ~~River~~rivers, converge at the Jacuí Delta, forming a substantial estuary that leads to the Guaíba River (**Figure 1b**).

The Guaíba River, an important freshwater system in ~~Rio Grande do Sul~~RS, plays a key role in providing drinking water, supporting navigation, and facilitating irrigation for the area. Located adjacent to Porto Alegre, the state capital, it has an average~~d~~ depth of 2 meters, with certain spots reaching over 30 meters near its outlet to the Patos Lagoon. Spanning approximately 10 km in width and 50 km in length, the river covers roughly 480 km².

Water from the Guaíba River flows into the Patos Lagoon, which stretches across a considerable area (250 km in length and 40 km in width), with an average depth of 5 meters, before connecting to the coastal ocean. Consequently, tidal fluctuations influence the downstream water levels in the Patos Lagoon basin. Furthermore, wind forces significantly impact both the Patos Lagoon and the Guaíba River, with prevailing winds oriented in a NE-SW direction across the state. The wind changes the water level in both systems, with SW (NE) wind restricting (facilitating) Guaíba flow into the Patos Lagoon, increasing (decreasing) Guaíba water levels up to 50 cm (Collischonn et al., 2025; Laipelt et al., 2025).

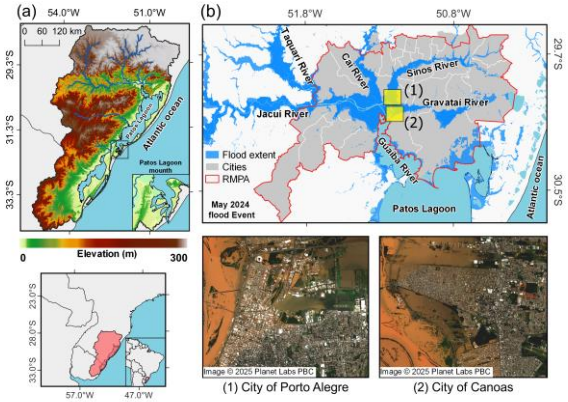

Figure 1: The Patos Lagoon basin, located in southern Brazil, features a mouth that connects to the Atlantic Ocean (a). The basin is fed by several primary tributaries, including the Taquari, Jacuí, Gravataí, Sinos, and Caí (b). These rivers experienced unprecedented flooding during the event in May 2024, affecting densely populated areas such as the state's capital, Porto Alegre, and cities in the Metropolitan Region of Porto Alegre (RMPA).

3. Material and methods

3.1. Simulation domain, boundary conditions and inputs

The simulation employed a two-dimensional (2D) hydrodynamic model based on the shallow water equations, accounting for inertia, gravity, friction, pressure, turbulent viscosity, wind and Coriolis effects. The model domain covers 23,000 km² (**Figure 2b**), corresponding to a 650 km reach from the upstream Jacuí to the Patos Lagoon's ocean outlet. This extent was defined based on available streamflow observations from the flood event. To ensure accuracy at the downstream boundary, the domain also includes a 45 km portion of the ocean, which is necessary to properly represent tidal effects influencing the lagoon.

Upstream boundary conditions were defined using streamflow time series for the main rivers of the Patos Lagoon basin, acquired from the Brazilian Water and Sanitation Agency (ANA) network (https://www.snirh.gov.br/hidrotelemetria/, accessed in July, 2024) (**Figure 2a**; **Supplementary Table 1**). The downstream boundary condition used tidal level time series from the Brazilian coast monitoring system (SIMCosta) network (https://simcosta.furg.br/home, accessed in August, 2024), located at the Patos Lagoon mouth. This ensures that the representation of the water levels over the basin are realistically subjected to the backwater effects of the tides under variable marine conditions. We did not incorporate auxiliary data for the minor tributaries, as their contributions were considered negligible compared to the primary river flows.

Formatted: Font: Bold

Formatted: Font: Not Bold

The simulation period ranged from April 28, 2024, to June 1, 2024, including a 10-day initial period for model warm-up. We implemented a variable-resolution mesh, using a 100-meter grid for primary rivers and floodplains, and a 500-meter grid for upland areas to optimize computational efficiency.

Surface topography was represented using the ANADEM Digital Terrain Model (DTM) product from ANA. ANADEM is a freely available DTM for South America derived from the COPERNICUS GLO-30 DEM (AIRBUS, 2020), removing vegetation bias using machine learning and satellite altimetry data (Laipelt et al., 2024).

To improve the hydraulic representation, the ANADEM DTM was modified to incorporate bathymetry from multiple sources. For the Jacuí, Gravataí, Sinos and Caí rivers, we used an interpolated bathymetry based on cross sections from publicly available data, as developed and validated by François (2021). For the Taquari River, where data was insufficient, the DTM was adjusted by lowering the channel elevation by approximately 4 meters between the upstream boundary condition and its confluence with the Jacuí River. Bathymetry for the Guaíba River and Patos Lagoon was derived from digitized nautical charts provided by the Board Hydrography and Navigation of the Brazilian Navy. Finally, ocean bathymetry from the General Bathymetric Chart of the Oceans (GEBCO) version 2024 (GEBCO, 2024) was integrated into the DTM to improve the representation of tidal dynamics in the Patos Lagoon estuary.

Wind data from the National Meteorological Institute of Brazil (INMET) (https://bdmep.inmet.gov.br/, accessed in August, 2024) were incorporated, as wind significantly impacts water levels in the Patos Lagoon and Guaíba River (Laipelt et al., 2025). The effect of the wind was computed using a drag formulation (Hsu, 2003), which modifies the aerodynamic roughness length by assuming a logarithmic velocity profile.

Initial values of Manning's roughness coefficient were derived from the literature and refined through manual calibration for the study period. Previous studies have modelled Patos Lagoon basin using Manning coefficients between 0.015 to 0.04 (António et al., 2020; Hillman et al., 2007; Marques et al., 2009; Martins and Fernandes, 2004), while values for the Guaíba River have ranged from 0.025 to 0.040 (Marques et al., 2009; Possa et al., 2022; Seiler et al., 2020). In the absence of specific data, the calibration of Manning's coefficient for the main channel was based on general hydrodynamic applications (Chow, 1959). For the floodplain, Manning's roughness coefficient values were calibrated by testing a range from 0.05 to 0.15, following the HEC-RAS manual guidelines (USACE, 2016).

A set of Manning's values evaluated for the 2D hydrodynamic model is presented in **Supplementary Table 2**, with statistical performance demonstrated in **Supplementary Figure 1**. Group 1 was selected for the simulations due to its higher accuracy, with calibrated values varying from 0.025 to 0.035, for the main channels, and 0.08 to 0.15 for floodplains.

Formatted: Normal, No bullets or numbering

Formatted: Font: Bold

Formatted: Normal, No bullets or numbering

Formatted: Font: Bold

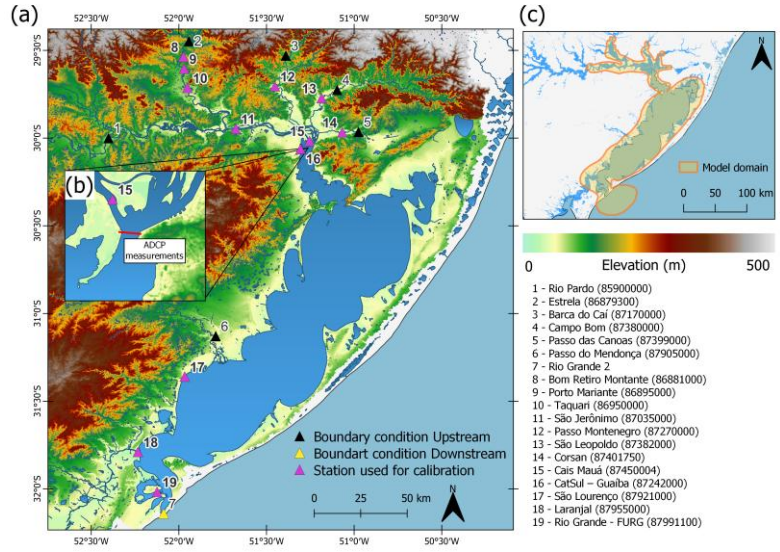

Figure 2: The locations and corresponding names of the gauge stations used for upstream conditions (black markers), downstream conditions (yellow markers), and calibration/validation (pink markers) are shown in (a). The ADCP measurement's location is identified by the red line in (b). The delineated geometry area (yellow) used for the two-dimensional simulation is shown in (c).

~~**For the two-dimensional simulation of the flood, we used the ANADEM Digital Terrain Model (DTM) product provided by the Brazilian Water and Sanitation Agency (ANA). ANADEM is a freely available DTM for South America that was obtained from the COPERNICUS GLO-30 DEM provided by the European Spatial Agency (ESA)**~~

3.2. Observational datasets and validation metrics

To evaluate ~~the accuracy of the two-dimensional hydrodynamic model~~model accuracy, we ~~performed a validation~~validated ~~of~~ water levels, streamflow, and flood extent. ~~We utilized water~~Water level validation utilized time series from independent gauge stations from ANA (~~situated across the study area, as outlined in~~ **Figure 2a**; ~~(more details in~~ **Supplementary Table 3**), which were ~~excluding stations used for~~not used for model boundary conditions. We incorporated

Formatted: List Paragraph, Indent: Left: 0.63 cm, Space Before: 0 pt, No bullets or numbering

Formatted: Heading 1, Space Before: 12 pt

Formatted: Normal, No bullets or numbering

~~The hydrodynamic model's~~o ~~performance was also evaluated using~~bservations from the Surface Water and Ocean Topography (SWOT) mission ~~observations~~ (Biancamaria et al., 2016; Durand et al., 2010; Fu et al., 2024)~~.~~ as ~~previous studies have shown~~ ~~that~~ SWOT has been previously shown to adequately represent this ~~data adequately represented the flood~~ event (Laipelt et al., 2025)~~. (Laipelt et al., 2025).~~ SWOT, a ~~is a~~ CNES/NASA collaboration~~collaborative effort between the Centre Nacional d'Études Spatiales (CNES) and the National Aeronautics and Space Administration (NASA),~~ is a radar interferometry sensor and provides instantaneous observations of water surface elevation (WSE)~~ing high-resolution data for oceans and inland water bodies (rivers, lakes, reservoirs and wetlands). Equipped with a Ka-band interferometer sensor, SWOT provides instantaneous observations of water surface elevation (WSE)~~ and water slope for rivers wider than 100 meters, ~~,~~with a revisit frequency of 21 days.

The ~~accuracy of the flood extent generated~~simulated flood extent accuracy ~~by the two-dimensional model~~ was verified ~~using~~against a high-resolution (5 m), clear-sky ~~image captured on May 6, 2024, near the peak flow over the RMPA. This image was captured by the~~ Planet RapidEye ~~constellation~~image captured near the flood peak on May 6, 2024 (Planet Team, 2024). The observed flood extent was then determined by ~~which provides imagery with spatial resolution of 5 meters per pixel and includes four multispectral bands (blue, green, red, and infrared). To determine the flood extent from the Planet image, we calculated~~calculating the Normalized Difference Water Index (NDWI) using **Equation 1**:

$$NDWI = \frac{(\alpha_{green} - \alpha_{infrared})}{(\alpha_{green} + \alpha_{infrared})} \quad (1)$$

where α_{green} is the green band and $\alpha_{infrared}$ is the infrared band.

To ensure compatibility, we resampled both the satellite flood extent and the model simulation output to a common 30-meter grid. We then calculated the relative extent ratio (**Equation 2)** between the simulate flood extent and observed by the satellite data.

$$H = 100\% \frac{P_{sim} \cap P_{obs}}{P_{obs}} \quad (2)$$

where P_{sim} is the number of flood pixels obtained from the simulation and P_{obs} the number of flood pixels identified with satellite imagery.

~~The accuracy of the S~~simulated streamflow accuracy was evaluated ~~by comparing it to~~against six~~6~~ field measurements ~~conducted using~~obtained using an Acoustic Doppler Current Profile (ADCP) instrument between May 5, 2024, and May 31, 2024 (Andrade et al., 2024; Silva et al., 2024b) ~~. The measurements were collected from two areas close to the~~collected near the Cais Mauá station ~~site~~ (**Figure 2c**~~;~~ ~~and the results are displayed in Table~~**Supplementary Table 4**~~1),~~ ~~, and more details can be found in~~ (Andrade et al., 2024)~~.~~.

Measurements on ~~days~~May 5 and 6 were ~~made~~obtained at the cross section of "Ponta da cadeia", while subsequent measurements (May ~~on days~~ 9 to~~o~~ 31) were ~~made 8 km downstream, at the cross section of the~~at the "Ponta do Dionísio" cross-section, 8 km downstream. The ~~Measurements at the~~ "Ponta da cadeia" measurements are like~~possib~~ly underestimate~~sions~~ of ~~the~~ total ~~river streamflow~~flow, ~~since on days 5 and 6 water was flowing over the~~as significant overbank flow was bypassing this cross-section on those dates.

Formatted: Font color: Black

Formatted: Indent: Left: 0.63 cm, No bullets or numbering

Formatted: Normal, No bullets or numbering

Formatted: Font: Bold

Formatted: Font: Not Bold

Model performance for water level was quantified using the Root Mean Square Error (RMSE), the Nash-Sutcliffe Efficiency coefficient (NSE) and the Mean Average Error (BIAS), as showed in **Equations 3**, **4** and **5**, respectively. To compare with the observations, the water level time series of the model were extracted from the simulation at the locations corresponding to the gauge stations.

~~floodplains west of the main river, and over the islands of the Jacuí Delta region, by passing the "Ponta da cadeia" cross section.~~

~~Table 1: Gauge station used for calibration of the model as well as its location. Source:~~

~~Date~~	~~Streamflow (m^3/s)~~	~~Cross section~~
~~5 May 2024~~	~~30,180~~	~~Ponta da cadeia~~
~~6 May 2024~~	~~29,852~~	~~Ponta da cadeia~~
~~9 May 2024~~	~~23,000~~	~~Ponta do Dionísio~~
~~15 May 2024~~	~~22,069~~	~~Ponta do Dionísio~~
~~22 May 2024~~	~~8,355~~	~~Ponta do Dionísio~~
~~31 May 2024~~	~~7,989~~	~~Ponta do Dionísio~~

~~The following metrics were used for the water level model's performance: Root Mean Square Error (RMSE), the Nash-Sutcliffe Efficiency coefficient (NSE) and the Mean Average Error (BIAS), as showed in **Equations 2**, **3** and **4**, respectively. To compare with the observations, the water level time series of the model were extracted from the simulation at the locations corresponding to the gauge stations.~~

$$RMSE = \frac{1}{2}\sqrt{\sum_{i=1}^{n}(O_i - P_i)^2} \quad (23)$$

$$NSE = 1 - \frac{\sum_{i=1}^{n}(O_i - P_i)^2}{\sum_{i=1}^{n}(O_i - \overline{O_i})^2} \quad (34)$$

$$BIAS = \frac{1}{n}\sum_{i=1}^{n}(O_i - P_i) \quad (45)$$

where O_i is the observed and P_i the predicted values and n the number of samples.

~~The flood extent produced by the two-dimensional model was validated by comparing the percentual pixels agreement to the water mask satellite observation based on **Equation 5**. To ensure compatibility, we adjusted the satellite flood extent's spatial resolution to 30 meters, aligning it with the simulation-generated flood extent.~~

$$H = 100\% \frac{P_{sim} \cap P_{obs}}{P_{obs}} \quad (5)$$

~~where P_{sim} is the number of flood pixels obtained from the simulation and P_{obs} the number of flood pixels identified with satellite imagery.~~

Formatted: Font:
Formatted: Normal, No bullets or numbering
Formatted: Font: Not Bold
Formatted: Indent: Left: 0.63 cm, No bullets or numbering
Formatted: Font: Not Bold
Formatted: Normal, No bullets or numbering
Formatted: Indent: Left: 0.63 cm, No bullets or numbering
Formatted: Normal, No bullets or numbering
Formatted: Indent: Left: 0.63 cm, No bullets or numbering
Formatted: Normal, No bullets or numbering

3.3. Experiment design overview

Figure 3 summarizes the study's methodological workflow. We simulated the May 2024 flood using the HEC-RAS software (version 6.4.1) (USACE, 2016), which was driven by publicly available data (topography, bathymetry, upstream inflow and weather).

First, a calibrated baseline model was established to accurately represent the event. Using this baseline, we then designed several experiments to better understand the basin's hydrodynamic processes during an extreme flood event. These experimental designs are detailed below.

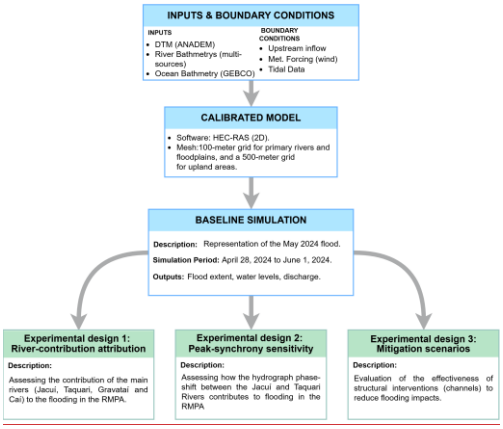

Figure 3. The workflow for this study proceeded by defining the input and boundary conditions for the May 2024 flood, followed by calibrating and validating a baseline model, which was then utilized to analyse multiple scenarios.

3.3.1. Baseline simulations

The baseline simulation represents the calibrated model of the May 2024 flood event, incorporating all observed data, including river inflows, tides, wind, and bathymetries described in Section 3.1.

3.3.2. River-contribution attribution

We used attribution scenarios to evaluate how individual tributaries influence flooding in the RMPA region. Specifically, we simulated four scenarios based on the baseline model, each excluding the streamflow from one main river (Jacuí, Taquari, Sinos, or Caí) to quantify its specific impact on water levels. This approach was selected because flood wave propagation is a

Formatted: Normal, Space Before: 0 pt, No bullets or numbering

Formatted: Font: Bold

Formatted: Normal, Space Before: 0 pt, No bullets or numbering

Formatted: Font: Bold

Formatted: Normal, Centered, Space Before: 0 pt, No bullets or numbering

Formatted: Normal, Space Before: 0 pt, No bullets or numbering

Formatted: Normal, Space Before: 0 pt, No bullets or numbering

non-linear process in the system, with its velocity governed by the system's channel geometry, roughness, and by the influence of the floodplains.

3.3.3. Peak-synchrony sensitivity

This analysis evaluated the combined flood impact of the Jacuí and Taquari rivers on the RMPA, considering the context of previous events. In May 2024, two cold fronts of varying spatial extent and intensity passed over the region between April 27 and May 2. As a consequence, the synchrony between the peak flows of major tributaries and the estuary-lagoon water level is a primary determinant of flood severity, directly informing the timing and feasibility of structural and operational measures. Given their distinct flow propagation times, we simulated a theoretical worst-case scenario by shifting the Jacuí River hydrograph (at Rio Pardo) forward by approximately 4 days to force their flood peaks arrive simultaneously. This synchronization allowed us to evaluate the potential consequences for the region's flood protection systems.

3.3.4. Mitigation scenarios

We tested proposed mitigation interventions currently under public and environmental agencies debate. Specifically, these proposals, which have not yet been formally evaluated, suggest the construction of new channels to reduce regional water levels in RMPA (DRRS, 2024; Hunt et al., 2024). Although these projects are still in the conceptual stage, we used the 2D hydrodynamic model to test their potential effects. This exercise aims to better comprehend the dominant forces controlling the system's dynamics.

For each proposed intervention, we evaluated three channel widths: 100-meter, 250-meter, and 500-meter. The channels were assigned a Manning's roughness of 0.02 and were integrated into the DTM. Additionally, a refined 50-meter mesh was used in these intervention areas.

The following scenarios for flood control were tested:

Channel connecting Jacuí to Guaíba: This experiment (**Figure 4a**) investigated the construction of a 7000-meter-long open channel connecting the Jacuí and Guaíba rivers. Its depth was adjusted based on the upstream and downstream river bathymetric data.

Channel connecting Patos Lagoon to the Ocean: This experiment (**Figure 4b**) investigated the efficiency of a hypothetical 17,000-meter-long and 10-meter-deep open channel connecting the northeastern part of the lagoon to the Atlantic Ocean. The downstream boundary for this channel used a tidal time series from the nearby SIMCosta network (tide gauge: Tramandaí; lon: -50.128; lat: -30.005) unaffected by the flood. Because this gauge lacks a precise altimetric reference, we estimated a correction factor by comparing its data to the referenced Rio Grande gauge (at the main lagoon outlet) during a non-flood period (May 2023–March 2024).~~To evaluate alternatives for mitigating flooding in the RMPA, we utilized the validated 2D model of the May flood event and designed two distinct hydraulic interventions in the studied region to test their efficacy. The location and evaluation of two channel openings were based on suggestions from studies as flood mitigation measures for future events in the RMPA , despite the absence of further efficacy evaluations.~~

Formatted: Normal, Space Before: 0 pt, No bullets or numbering

Formatted: Heading 1, Space Before: 12 pt

Formatted: Normal, No bullets or numbering

Formatted: Font: Bold

Formatted: Font: Bold

Formatted: Font: Bold

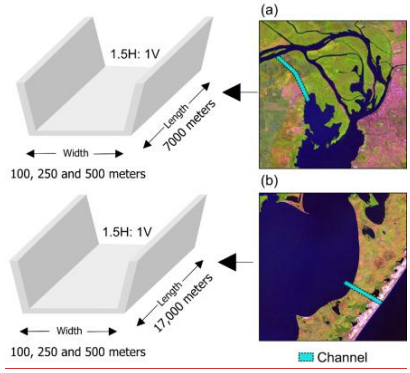

Figure 4: Evaluation of two hydraulic structures scenarios for flood control in RMPA: (a) an open channel connecting Jacuí and Guaíba rivers, and (b) a channel connecting Patos Lagoon to the Atlantic Ocean.

4. Results

4.1. Model Validation

4.1.1. Water level

Figure 5 shows a comparison between simulated water levels from the two-dimensional hydrodynamic model and measurements from gauge stations and SWOT. The simulation accurately captured the flow peak at most stations, showing an average BIAS of -0.47 meters in the water level peak. The BIAS ranged from -2.17 meters in the Bom Retiro station to 0.36 meters in the Taquari station. Conversely, the simulation failed to capture low flow at the Taquari River stations, exhibiting difference of -3.5 meters and -3.4 meters for Bom Retiro and Porto Mariante stations, respectively. This suggests an inconsistency in the representation of the river's man channel in the DTM.

Performance metrics revealed an average NSE of 0.82, with a range of 0.68 to 0.92. The RMSE averaged 0.71 meters, with values ranging from 0.10 to 1.68 meters. Differences between simulated and observed water levels exhibited relatively low BIAS, ranging from -0.2 to 0.82 meters, with an overall average below 0.07 meters. An exception was noted at the Cais Mauá gauge station, where official records diverged from the simulation after May 15. This discrepancy is explained as a measurement error resulting from the emergency relocation of the station due to flood damage (Collischonn et al., 2024). To ensure accurate flood representation at the location, the simulation was also compared with data from a nearby experimental station (https://www.tidesatglobal.com/, accessed in September 2024). This comparison yielded a consistent agreement with the overall results (NSE = 0.85; RMSE = 0.32 meters; BIAS = -0.12 meters). Nevertheless, the metrics obtained demonstrated

Formatted: Centered

Formatted: Outline numbered + Level: 1 + Numbering Style: 1, 2, 3, … + Start at: 1 + Alignment: Left + Aligned at: 0 cm + Indent at: 0.63 cm

Formatted: Outline numbered + Level: 2 + Numbering Style: 1, 2, 3, … + Start at: 1 + Alignment: Left + Aligned at: 0 cm + Indent at: 0.63 cm

Formatted: Outline numbered + Level: 3 + Numbering Style: 1, 2, 3, … + Start at: 1 + Alignment: Left + Aligned at: 0 cm + Indent at: 0.63 cm

the essential requirements for a hydrodynamic model capable of providing locally relevant estimates (Fleischmann et al., 2019).

Additionally, the study compared simulated water levels with SWOT observations during the flood event. Both representations aligned well with water level observations from stations. The comparison between the simulation and SWOT observations revealed an average BIAS of 0.13 meters. SWOT data effectively captured water level variations along the main rivers of the Patos Lagoon basin, providing valuable validation for hydrodynamic simulations. **Figure 6** displays a profile line obtained by SWOT on May 6th, (near the peak in the RMPA), compared with the simulation for the same overpass (~11h a.m.) between the Jacuí River and Guaíba rivers. Both results exhibited similar water slopes, with SWOT observed a slope of 7.05 cm/km, while the 2D simulation indicated a slope of 6.45 cm/km. These findings underscore the severity of the flood event, as the water slope increased by almost 10 times compared to low-flow conditions.

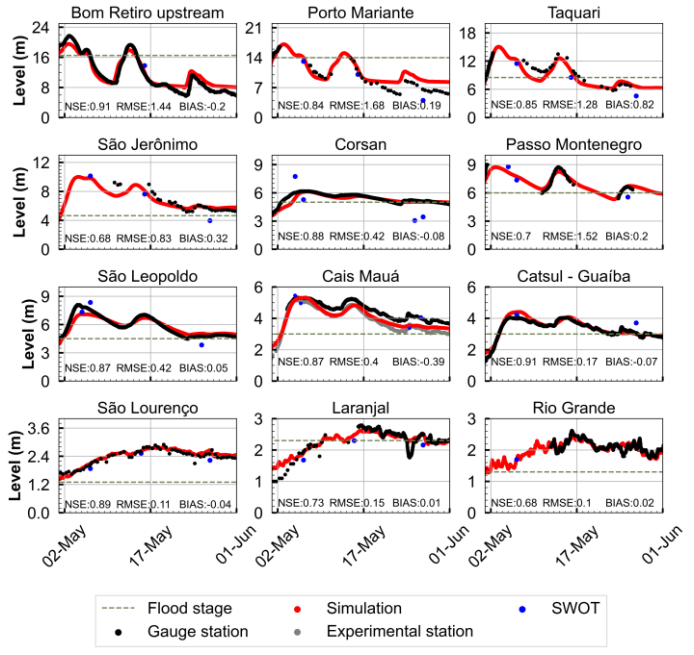

Formatted: Centered

Figure 5: Water level simulations (red) compared to observations at twelve gauge stations observations (black) located in the study area, alongside water surface elevation (WSE) data from the SWOT mission (blue). The grey line in the Cais Mauá plot corresponding to the experimental site data, and the dashed line indicates the flood stage at each station.

~~2.~~

~~1.1. Digital terrain model and bathymetry~~

~~For the two-dimensional simulation of the flood, we used the ANADEM Digital Terrain Model (DTM) product provided by the Brazilian Water and Sanitation Agency (ANA). ANADEM is a freely available DTM for South America that was obtained from the COPERNICUS GLO-30 DEM provided by the European Spatial Agency (ESA) by removing vegetation bias .~~

~~To enhance the representation of the water bodies in the hydrodynamic simulation, modifications were implemented in the ANADEM product. For the Jacuí, Gravataí, Sinos and Caí Rivers, an interpolated bathymetry based on cross sections from different publicly available data was used, developed and validated by . Due to insufficient data for the Taquari River, we reduced the water elevation in the MDT by approximately 4 meters between the upstream boundary condition and the confluence with the Jacuí River, based on manually calibration. The bathymetry for the Guaíba River and Patos Lagoon was derived from digitalized nautical charts provided by the Board Hydrography and Navigation of the Brazilian Navy. Lastly, we incorporated the ocean bathymetry from the General Bathymetric Chart of the Oceans (GEBCO) version 2024 into the MDT to improve the representation of tidal dynamics in the Patos Lagoon estuary.~~

~~1.2. HEC-RAS model~~

~~We utilized HEC-RAS software (version 6.4.1) , developed by the U.S. Army Corps of Engineers, to simulate the May 2024 flood in the RMPA. The domain area coverage an area of 23,000 km² corresponding to a 650 km reach between upstream Jacuí and the Patos Lagoon outlet to the ocean. It was defined based on streamflow observations available during the flood event. Additionally, we included a 45 km portion of the ocean to represent the tidal effect in the simulation.~~

~~The simulation employed a two-dimensional hydrodynamic representation based on the shallow water equations. This model accounts for inertia and forces related to gravity, friction, pressure, turbulent viscosity, wind and Coriolis effects.~~

~~The simulation period ranged from April 28, 2024, to June 1, 2024, including a 10-day initial period for model spin up. We implemented a variable mesh resolution (Figure 2b), applying a 100-meter grid for primary rivers and floodplains, and a 500-meter grid for upland areas to enhance computational efficiency.~~

~~As upstream boundary condition, we used discharge time series from the main rivers of the the Patos Lagoon Basin. Data were acquired from the Brazilian Water and Sanitation Agency (ANA) network (https://www.snirh.gov.br/hidrotelemetria/, accessed in July, 2024) (Figure 2a). Detailed information is provided in Supplementary Table 1. For the downstream boundary condition, we utilized tidal level time series from the Brazilian coast monitoring system (SIMCosta) network (https://simcosta.furg.br/home, accessed in August, 2024), located at the Pato Lagoon mouth, which connects to the Atlantic Ocean.~~

~~For meteorological inputs, we incorporated wind data from the National meteorological Institute of Brazil (INMET) (https://bdmep.inmet.gov.br/, accessed in August, 2024) to represent its impact on the Patos Lagoon and Guaíba River.~~

Formatted: Font: Not Bold

Formatted: Font: Not Bold

Formatted: Font: Not Bold

Formatted: Font: Not Bold

Formatted: Font: Not Bold

Formatted: Normal, Space Before: 0 pt, No bullets or numbering

Formatted: Outline numbered + Level: 2 + Numbering Style: 1, 2, 3, … + Start at: 1 + Alignment: Left + Aligned at: 0 cm + Indent at: 0.63 cm

Formatted: Heading 1, Space Before: 12 pt

Formatted: Space Before: 12 pt, No bullets or numbering

Formatted: Heading 1, Space Before: 12 pt

~~Winds forces in the simulation were computed based on Eulerian method and using drag formulation, which assumes a logarithmic wind velocity profile, modifying the aerodynamic roughness length in the simulation.~~

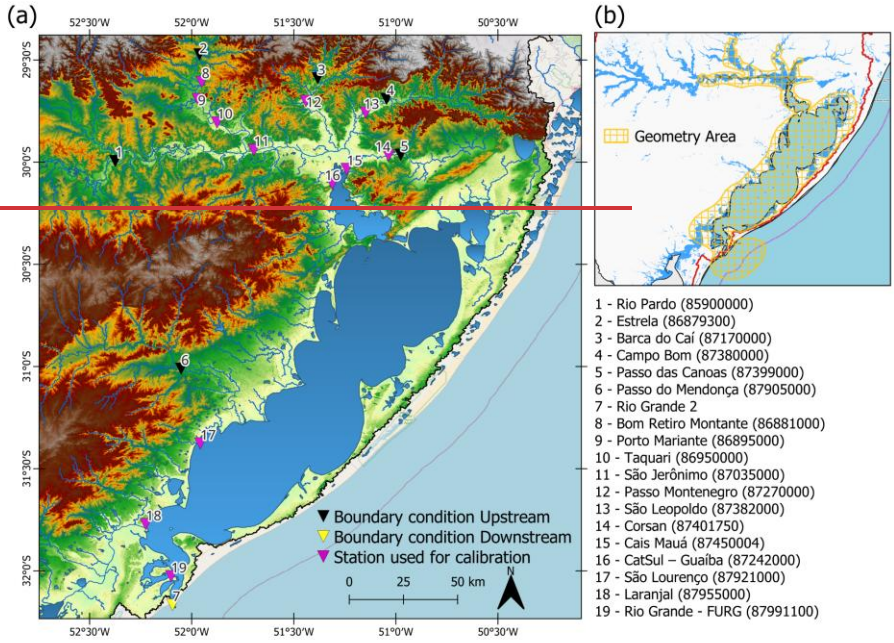

~~Figure 2: The locations and corresponding names of the gauge stations used for upstream conditions (black markers), downstream conditions (yellow markers), and calibration/validation (pink markers) are shown in (a). The delineated geometry area (yellow) used for the two-dimensional simulation is shown in (b).~~

~~Initial values of Manning's roughness coefficient were derived from the literature, followed by manual calibration for the study period to ensure optimal accuracy. Supplementary Table 2 presents the Manning's roughness values utilized in this study, varying between 0.025 to 0.035 for the main channel and 0.08 to 0.3 for the floodplains. Prior studies have modelled Patos Lagoon basin using Manning coefficients between 0.015 to 0.04 , while values for the Guaíba River have ranged from 0.025 to 0.040 . In the absence of specific data, the calibration of Manning's coefficient for the main~~

Formatted: Heading 1, Left, Space Before: 12 pt

Formatted: Heading 1, Space Before: 12 pt

~~channel was based on general hydrodynamic applications . For the floodplain, Manning's roughness coefficient values were calibrated by testing a range from 0.05 to 0.15, following the HEC-RAS manual guidelines .~~

~~1.3. Water level, streamflow and flood extent validation~~

~~To evaluate the accuracy of the two-dimensional hydrodynamic model, we performed a validation of water levels, streamflow, and flood extent. We utilized water level time series from independent gauge stations situated across the study area, as outlined in Figure 2a (more details in Supplementary Table 3), excluding stations used for boundary conditions.~~

~~The hydrodynamic model's performance was also evaluated using Surface Water and Ocean Topography (SWOT) observations , as previous studies have shown that SWOT data adequately represented the flood event (Laipelt et al., 2025). SWOT is a collaborative effort between the Centre Nacional d'Études Spatiales (CNES) and the National Aeronautics and Space Administration (NASA), providing high-resolution data for oceans and inland water bodies (rivers, lakes, reservoirs and wetlands). Equipped with a Ka-band interferometer sensor, SWOT provides instantaneous observations of water surface elevation (WSE) and water slope for rivers wider than 100 meters, with a revisit frequency of 21 days.~~

~~The accuracy of the flood extent generated by the two-dimensional model was verified using a high-resolution, clear-sky image captured on May 6, 2024, near the peak flow over the RMPA. This image was captured by the Planet RapidEye constellation which provides imagery with spatial resolution of 5 meters per pixel and includes four multispectral bands (blue, green, red, and infrared). To determine the flood extent from the Planet image, we calculated the Normalized Difference Water Index (NDWI) using Equation 1:~~

$$NDWI = \frac{(\alpha_{green} - \alpha_{infrared})}{(\alpha_{green} + \alpha_{infrared})} \quad (1)$$

~~where α_{green} is the green band and $\alpha_{infrared}$ is the infrared band.~~

~~The accuracy of the simulated streamflow was evaluated by comparing it to 6 field measurements conducted using an Acoustic Doppler Current Profile (ADCP) instrument between May 5, 2024, and May 31, 2024 . The measurements were collected from two areas close to the Cais Mauá station site, and the results are displayed in Table 1, and more details can be found in .~~

~~Measurements on days 5 and 6 were made at the cross section of "Ponta da cadeia", while measurements on days 9 to 31 were made 8 km downstream, at the cross section of the "Ponta do Dionísio". Measurements at the "Ponta da cadeia"~~

Formatted: Space Before: 12 pt, No bullets or numbering

Formatted: Heading 1, Space Before: 12 pt

~~are possibly underestimations of the total river streamflow, since on days 5 and 6 water was flowing over the floodplains west of the main river, and over the islands of the Jacuí Delta region, by passing the "Ponta da cadeia" cross section.~~

~~Table 1: Gauge station used for calibration of the model as well as its location. Source: and Andrade et al. (2024).~~

~~Date~~	~~Streamflow (m^3/s)~~	~~Cross section~~
~~5 May 2024~~	~~30,180~~	~~Ponta da cadeia~~
~~6 May 2024~~	~~29,852~~	~~Ponta da cadeia~~
~~9 May 2024~~	~~23,000~~	~~Ponta do Dionísio~~
~~15 May 2024~~	~~22,069~~	~~Ponta do Dionísio~~
~~22 May 2024~~	~~8,355~~	~~Ponta do Dionísio~~
~~31 May 2024~~	~~7,989~~	~~Ponta do Dionísio~~

~~1.4. Performance metrics~~

~~The following metrics were used for the water level model's performance: Root Mean Square Error (RMSE), the Nash-Sutcliffe Efficiency coefficient (NSE) and the Mean Average Error (BIAS), as showed in Equations 2, 3 and 4,~~

Formatted: Heading 1, Left, Space Before: 12 pt

Formatted: Heading 1, Left, Space Before: 12 pt

Formatted: Heading 1, Left, Space Before: 12 pt

Formatted: Heading 1, Left, Space Before: 12 pt

Formatted: Heading 1, Left, Space Before: 12 pt

Formatted: Heading 1, Left, Space Before: 12 pt

Formatted: Heading 1, Left, Space Before: 12 pt

Formatted: Space Before: 12 pt, No bullets or numbering

Formatted: Heading 1, Space Before: 12 pt

~~respectively. To compare with the observations, the water level time series of the model were extracted from the simulation at the locations corresponding to the gauge stations.~~

~~$$RMSE = \frac{1}{2}\sqrt{\sum_{i=1}^{n}(O_i - P_i)^2} \quad (2)$$~~

~~$$NSE = 1 - \frac{\sum_{i=1}^{n}(O_i - P_i)^2}{\sum_{i=1}^{n}(O_i - \bar{O}_i)^2} \quad (3)$$~~

~~$$BIAS = \frac{1}{n}\sum_{i=1}^{n}(O_i - P_i) \quad (4)$$~~

~~where O_i is the observed and P_i the predicted values and n the number of samples.~~

~~The flood extent produced by the two-dimensional model was validated by comparing the percentual pixels agreement to the water mask satellite observation based on Equation 5. To ensure compatibility, we adjusted the satellite flood extent's spatial resolution to 30 meters, aligning it with the simulation-generated flood extent.~~

~~$$H = 100\% \frac{P_{sim} \cap P_{obs}}{P_{obs}} \quad (5)$$~~

~~where P_{sim} is the number of flood pixels obtained from the simulation and P_{obs} the number of flood pixels identified with satellite imagery.~~

~~1.5. Simulation experiments~~

Formatted: Space Before: 12 pt, No bullets or numbering

Formatted: Heading 1, Space Before: 12 pt

~~The first main result is the model validation itself, which calculate values were compared to level gauges, streamflow measurements, flood extensions and SWOT altimetry data. These results are followed by studies of the hydraulic mechanisms of the flood, which included the relevance of each river that drains to the Guaíba River water levels and the assessment of the synchronization of the water level peaks that reach the Guaíba River.~~

~~Finally, a set of hydraulic interventions experiments was organized. For each experiment, three scenarios were evaluated, varying the channel width from a feasible engineering solution for flood control (100-meter width) to a more challenging solution (500-meter width), with a median alternative (250-meter width). The channels were assigned a Manning's roughness coefficient of 0.02 and integrated into the MDT using HEC-RAS tools. Additionally, for these simulations, a refined mesh with a 50-meter cell size was used to model the intervention areas.~~

~~The following scenarios for flood control were tested:~~

~~Channel connecting Jacuí to Guaíba: This experiment investigated the construction of an open channel connecting the Jacuí and Guaíba River, as shown in Figure 3a. We tested multiple width scenarios (100, 250 and 500 meters), with 7000 meters in length, and its depth adjusted according to upstream and downstream bathymetric data for both rivers.~~

Formatted: Heading 1, Indent: First line: 0 cm, Space Before: 12 pt

~~Channel connecting Patos Lagoon to the Ocean: The second experiment involved designing a hypothetical open channel connecting the Patos Lagoon to the Atlantic Ocean in the northeastern part of the lagoon (Figure 3b). The length of the channel was defined as 17,000 meters, with and 10 meters in depth. In this evaluation, we used a tidal water level time series from SIMCosta network (tide gauge: Tramandaí; lon: -50.128; lat: -30.005) as the boundary condition at the channel's exit, which was obtained near the proposed channel location and unaffected by the influence of the flood. Due to the absence of an altimetric reference, a correction factor was estimated based on the difference between the Tramandaí series and the tide gauge data from Rio Grande in the Patos Lagoon outlet, which has an altimetric~~

reference. To estimate the correction factor, a different time interval was chosen to avoid the influence of the flood in the Rio Grande time series (between May 2023 and March 2024).

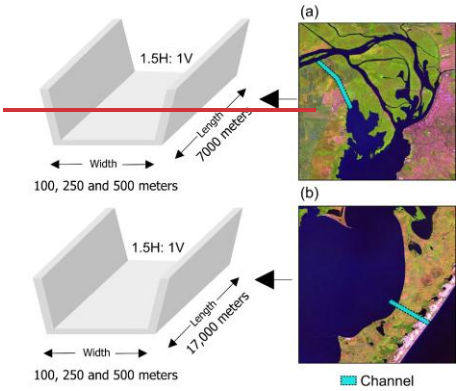

Figure 3: Three scenarios with different hydraulic structures were evaluated to mitigate flood in the RMPA. (a) An open channel connecting Jacuí and Guaíba River; (b) A channel connecting Patos Lagoon with the ocean.

2. Results and Discussion

2.1. Model Validation

Water level

Figure 4 shows a comparison between simulated water levels from the two-dimensional hydrodynamic model and measurements from gauge stations and SWOT. The simulation was able to capture the flow peak in most of the stations, showing an average BIAS of -0.47 meters between the water level peak in the stations, ranging from -2.17 meters in the Bom Retiro station to 0.36 meters in the Taquari station. On the other hand, low flow in the Taquari River stations were not captured by the simulation, with difference of -3.5 meters and -3.4 meters for Bom Retiro and Porto Mariante stations, respectively, suggesting an inconsistency with the representation of the river man channel in the MDT.

Performance metrics revealed an average NSE of 0.82, with a range of 0.68 to 0.92, The RMSE averaged 0.71 meters, with values ranging from 0.10 to 1.68 meters. Differences between simulated and observed water levels exhibited relatively low BIAS, ranging from -0.2 to 0.82 meters, with an overall average below 0.07 meters. An exception was noted at the Cais Mauá gauge station, where official records diverged from the simulation after May 15. This discrepancy is explained as a measurement error resulting from the emergency relocation of the station due to flood damage (Collischonn et al., 2024). To ensure accurate flood representation at the location, the simulation was also compared with data from a nearby experimental station (https://www.tidesatglobal.com/, accessed in September 2024), yielding a consistent agreement with the results (NSE=0.85; RMSE=0.32 meters; BIAS=−0.12 meters). Nevertheless, the

Formatted: Heading 1, Left, Space Before: 12 pt

Formatted: Heading 1, Space Before: 12 pt

Formatted: No bullets or numbering

Formatted: Heading 1, Space Before: 12 pt

~~metrics obtained demonstrated the essential requirements for a hydrodynamic model capable of providing locally relevant estimates .~~

~~Additionally, the study compared simulated water levels with SWOT observations during the flood event. Both representations aligned well with water level observations from stations. The comparison between the simulation and SWOT observations revealed an average BIAS of 0.13 meters. SWOT data effectively captured water level variations along the main rivers of the Patos Lagoon basin, providing valuable validation for hydrodynamic simulations. Figure 5 displays a profile line obtained by SWOT on May 6, (near the peak in the RMPA) compared with the simulation for the same overpass (~11h a.m.) between Jacuí River and Guaíba River. Both results exhibited similar water slopes, with SWOT observing a slope of 7.05 cm/km, while the 2D simulation indicated a slope of 6.45 cm/km. These findings~~

~~underscore the severity of the flood event, as the water slope increased by almost 10 times compared to low flow conditions.~~

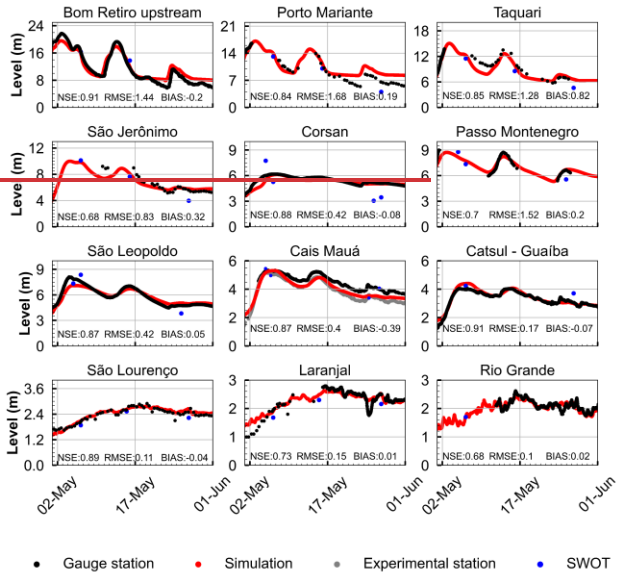

~~Figure 4: Water level simulations (red) compared to observations at nine-gauge stations observations (black) located in the study area. Water surface elevation (WSE) from the SWOT mission (blue). The grey line in the Cais Mauá plot corresponding to experimental.~~

Formatted: Heading 1, Left, Space Before: 12 pt

Formatted: Heading 1, Space Before: 12 pt

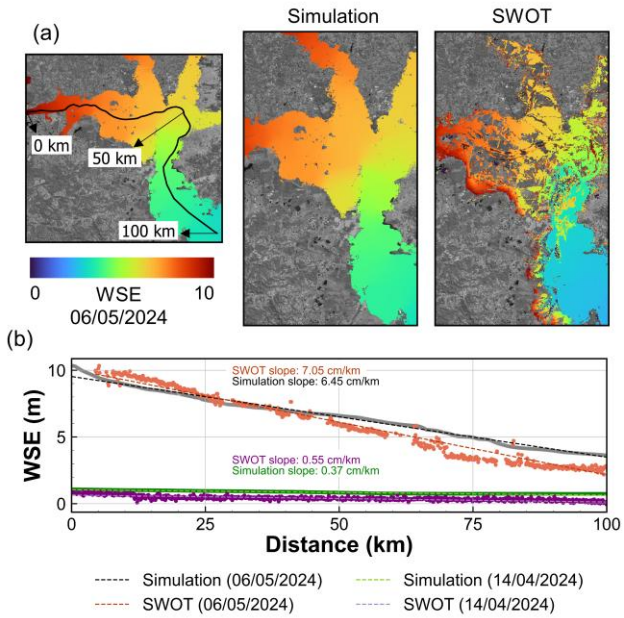

Figure ~~5~~6: ~~Water surface elevation (WSE~~Water surface elevation~~)~~ slope from the 2D simulation (a) compared with SWOT data observation from ~~6~~ May 6th. ~~for a~~ The profile line between Jacuí and Guaíba River (b) ~~b). Both results~~ showed steep water slope changes (SWOT = 7.05 cm/km and Simulation = 6.45 cm/km) compared to low waters stable conditions (SWOT = 0.55 cm/km and Simulation = 0.37 cm/km).

~~2.1.2.~~4.1.2. Flood extent

The comparison between the flood extent captured by high-resolution optical satellite imagery and that generated by the 2D simulation is presented in **Figure ~~6~~7**. While our validation was constrained to the flood extent within the simulation boundaries, excluding peripheral areas affected ~~beyond~~, the model exhibited strong agreement with the flood extent observed in the May 6 satellite images~~. The simulation achieved an~~, achieving 83% agreement ~~with the satellite data according to **Equation 5**~~. ~~Nevertheless~~However, this validation approach has certain limitations due to variations in peak flow across the basin. For instance, while the satellite image timing aligns closely with the peak water levels in the RMPA~~, but it~~, it was captured approximately 5 days after the upstream peak (e.g., Taquari River).

Formatted: Outline numbered + Level: 3 + Numbering Style: 1, 2, 3, … + Start at: 1 + Alignment: Left + Aligned at: 0 cm + Indent at: 0.63 cm

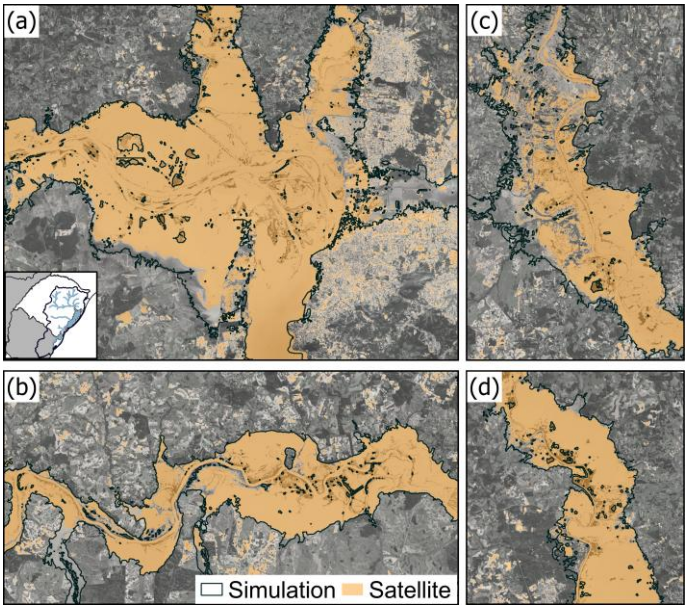

Figure ~~6~~7: Validation of the flood extent using ~~, based on~~ optical satellite images captured by the PlanetScope constellation on May 6, which was near the peak water levels in the RMPA. The simulated flood extent (indicated by the ~~blue~~ black line) ~~revealed a~~ closely matched the satellite observations. ~~, including in the areas of the RMPA (a), Jacuí River (b) and Taquari River (c)~~Illustration detail areas in the RMPA (a), the Jacuí River (b), the Taquari River (c) and the Caí River (d).~~.~~

~~2.1.3.~~4.1.3. Streamflow

Simulated streamflow was compared to field measurements collected during the flood event, as shown in **Figure** ~~7~~8. Measurements were collected from two nearby locations "Ponta do Dionísio" and "Ponta da cadeia" (**Figure** ~~7a~~8a). Due to ~~their~~ the proximity of both sections (~~around~~ approximately 6 km), and the similarity of their measurements, we only compared ~~the~~ simulation results ~~with~~ obtained at the "Ponta do Dionísio" ~~measurements~~location~~, as they were very similar~~. The results indicated that both the magnitude and temporal progression of the simulated streamflow ~~are~~ were similar to observations (**Figure** ~~7b~~8b). The observed peak streamflow ~~observed~~ was 30,180 m³/s on May 5 at 6:00 PM, while the simulation estimated 30,724 m³/s for the same time. The model's overall bias error was 1088 m³/s, corresponding to a percentage error of 5.4%. This error is below the ~~, which is under the~~ expected uncertainty for~~of a~~ measurements under ~~this~~ such extreme conditions

Formatted: Outline numbered + Level: 3 + Numbering Style: 1, 2, 3, … + Start at: 1 + Alignment: Left + Aligned at: 0 cm + Indent at: 0.63 cm

(McMillan et al., 2018). For individual sections, the average errors were 1062 m³/s and 1115 m³/s for “Ponta da cadeia” and “Ponta do Dionísio”, respectively.

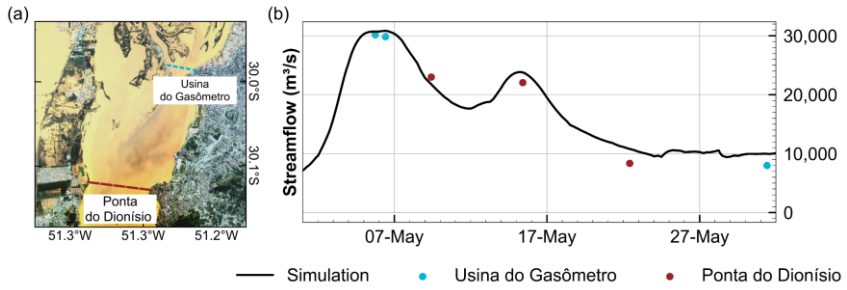

Figure ~~7~~8: Streamflow observations ~~were~~ collected during the 2024 flood in the Guaíba River with Acoustic Doppler Current Profiler (ADCP). Subplot (a) shows the measurements sections ~~instrument in the~~at Ponta do Dionísio (red dash line) and “Ponta da cadeia” (blue dash line) ~~sections (a)~~. Subplot (b) compare these o~~O~~bservations ~~were compared~~ with the streamflow simulation data from the two-dimensional model, ~~showing~~ demonstrating good agreement ~~(b)~~.

~~2.2.~~4.2. Hydraulic mechanisms of the flood

Formatted: Outline numbered + Level: 2 + Numbering Style: 1, 2, 3, … + Start at: 1 + Alignment: Left + Aligned at: 0 cm + Indent at: 0.63 cm

~~Based on the validated model, we simulated different scenarios in the RMPA to better understand the hydraulic mechanisms that influenced the event. The contribution of the main rivers to the flooding in the RMPA was analysed by eliminating each river's contribution to assess its impact on flooding levels. Additionally, a possible extreme scenario was simulated, in which the peak flood of the main rivers (Jacuí and Taquari) was synchronized.~~

~~2.2.2.~~4.2.1. River flood contribution

Formatted: Space Before: 0 pt, Outline numbered + Level: 3 + Numbering Style: 1, 2, 3, … + Start at: 1 + Alignment: Left + Aligned at: 0 cm + Indent at: 0.63 cm

The analysis revealed that the Jacuí and Taquari rivers are the primary contributors to RMPA flooding, ~~whereas~~ while the remaining rivers that flow into the Guaíba River (Caí, Gravataí, and Sinos) have a minimal effect on RMPA water levels ~~in general~~.

Our findings indicated that if the Taquari River's flood contribution were eliminated (**Figure** ~~8~~9, yellow line), the maximum water level would drop from 5.30 to 4.25 meters, highlighting the ~~Jacuí River's~~ critical~~l~~ role of the Jacuí River in RMPA flooding. This scenario would also ~~result in a~~ delay ~~of~~ the peak water level by approximately 4 days compared to the May flood event.

Conversely, removing the Jacuí River's contribution (**Figure** ~~8~~9, blue line) would make the Taquari River the primary contribution. The Taquari River's flow characteristics would cause the RMPA peak to occur earlier by about one day~~would~~

~~cause an earlier peak in the RMPA by about 1 day~~. Under these conditions, the peak water level would be lower, dropping from 5.30 ~~meters~~ to 4.75 meters. Furthermore, ~~, and~~ the flood behaviour would exhibit two peaks, ~~like the~~similar to the actual event (**Figure ~~8~~9**, black line), which is not observed ~~unlike the scenario where~~when the Taquari River's contribution was removed.

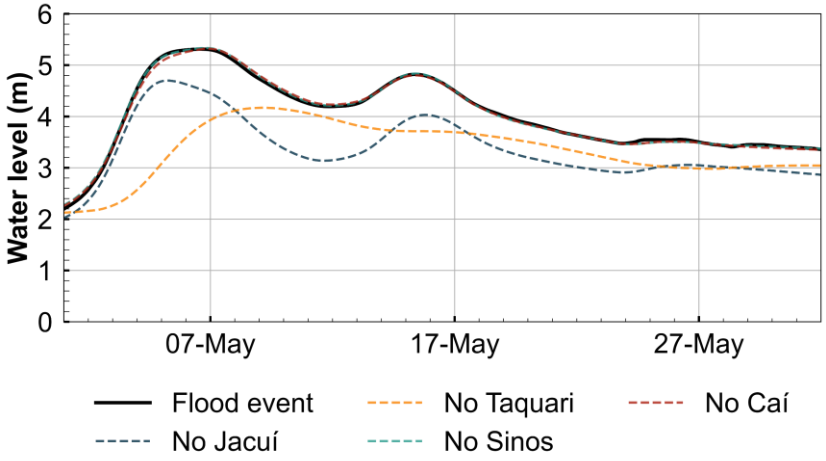

Figure ~~8~~9: ~~To evaluate the impact~~Impact of individual ~~each~~ river contributions on RMPA flooding, ~~we eliminated the contributions of individual rivers~~based on scenarios where each river's input was removed from the simulation (Taquari, Jacuí, Sinos, Gravataí, and Caí). T~~his analysis revealed that the~~he Jacuí and Taquari r~~R~~ivers are identified as the primary ~~contributors to flooding in the RMPA~~flood contributions. Excluding the Taquari River's input ~~during the May flood~~ would lower~~reduce~~ the peak flood level to 4.25 meters, while removing the Jacuí River's contribution would ~~result in a~~lower the peak ~~flood level of~~to 4.75 meters. In both scenarios, the peak flood level would still exceed the flood threshold for RMPA cities.

~~2.2.3.~~4.2.2. River flood synchronization

~~We accessed the contribution of Jacuí and Taquari Rivers for the flood in the RMPA. Considering that both rivers have distinct flow propagation regimes, we simulated a scenario in each both Jacuí and Taquari flood peaks would arrive at RMPA at the same time. After several testes, we anticipated the boundary condition hydrograph of the Jacuí River at Rio Pardo by approximately 4 days to represent maximum synchronization.~~

Formatted: Outline numbered + Level: 3 + Numbering Style: 1, 2, 3, … + Start at: 1 + Alignment: Left + Aligned at: 0 cm + Indent at: 0.63 cm

Figure ~~9~~ **10** presents ~~ed~~ the simulation results for the synchronized peak flood scenario of the Taquari and Jacuí rivers. This scenario~~,~~ indicates~~which indicate~~ an increase in the peak water level ~~peak in the RMPA~~ by 0.82 meters, ~~whereas~~ while the flood extent ~~in this scenario~~ would ~~have~~ increase by 8% over the study area. In this hypothetical scenario, maximum water levels could have ~~been~~ reached nearly 6 meters. This maximum~~,~~ level is ~~which is~~ equivalent to the estimated ~~to be the~~ ~~actual~~design maximum flood level of the protection system for~~of~~ the city of Porto Alegre.~~, the state's capital.~~

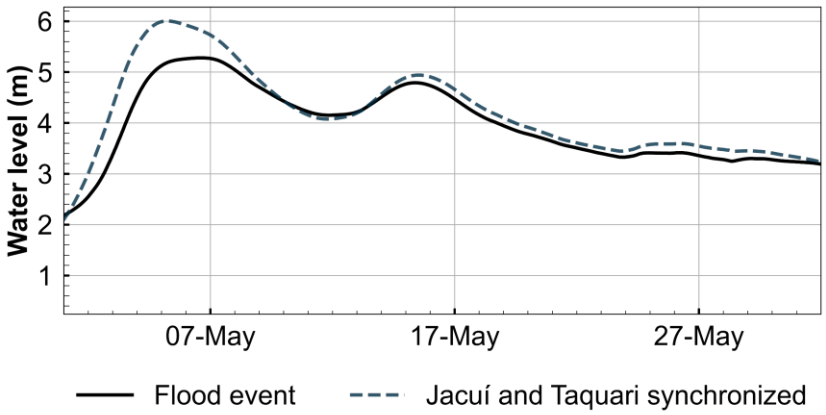

Figure ~~9~~**10**. Comparative of the flood event water level simulation (black line) and ~~synchronizing~~ synchronized water level peak of the Jacuí and Taquari Rivers ~~(grey dashed line)~~ arriving in Porto Alegre (grey dashed line). ~~In the RMPA, the~~The maximum water level peak in the RMPA increased to 6 meters, suggesting a worsened scenario that could potentially surpass flood control systems.~~.~~

~~4.3.~~ Hydraulic interventions for flood control

~~2.2.~~

~~2.2.5.~~4.3.1. Jacuí-Guaíba channel

Results from ~~the~~ this experiment ~~modelling the impact of a new~~ channel connecting the Jacuí and Guaíba ~~River~~ rivers ~~were analysed at specific locations within the study area~~are presented in **Figure 11**. At Point A (**Figure** ~~10a~~**11a**), located upstream ~~from~~ of the channel structure, the maximum water level decreased by 0.1~~0~~ meters for the 100-meter width scenario and 0.27 meters for the 500-meter width scenario. At Point B, ~~located~~ in the northeastern ~~part~~ portion of the Jacuí Delta (**Figure** ~~10b~~**11b**), the channel's effectiveness was less pronounced, resulting in water level reductions of 0.05 meters (100-meter width),

Formatted: Outline numbered + Level: 2 + Numbering Style: 1, 2, 3, … + Start at: 1 + Alignment: Left + Aligned at: 0 cm + Indent at: 0.63 cm

Formatted: Normal, Outline numbered + Level: 1 + Numbering Style: 1, 2, 3, … + Start at: 1 + Alignment: Left + Aligned at: 0 cm + Indent at: 0.63 cm

Formatted: Space Before: 0 pt, Outline numbered + Level: 3 + Numbering Style: 1, 2, 3, … + Start at: 1 + Alignment: Left + Aligned at: 0 cm + Indent at: 0.63 cm

Formatted: Font: Bold

0.12 meters (250-meter width), and 0.19 meters (500-meter width) across the evaluated scenarios. At~~Finally, at~~ the Cais Mauá station (Point C), ~~the flow peak in~~representing the Porto Alegre ~~showed minimal change~~reach (**Figure ~~10~~c~~11~~c**), the peak flow showed negligible variation, ~~-~~with the maximum water level decreasing by less than 0.10 meters in all ~~scenarios~~ tested scenarios.

~~Thus~~Overall, the proposed structural intervention to ~~reduce~~ lower water levels over the Guaíba River and the Jacuí Delta seems ineffective. The simulated reductions ~~Water level reduction~~ promoted by this intervention are small compared to the water level variation during the flood and compared to the model´s uncertainty range. Even~~ with~~ the widest channel configuration~~design~~ ~~—~~which ~~would~~ require the most significant engineering intervention and financial investment~~—~~ would~~the~~ result ins ~~show that water level reductions would be small~~only minor reduction in water levels.

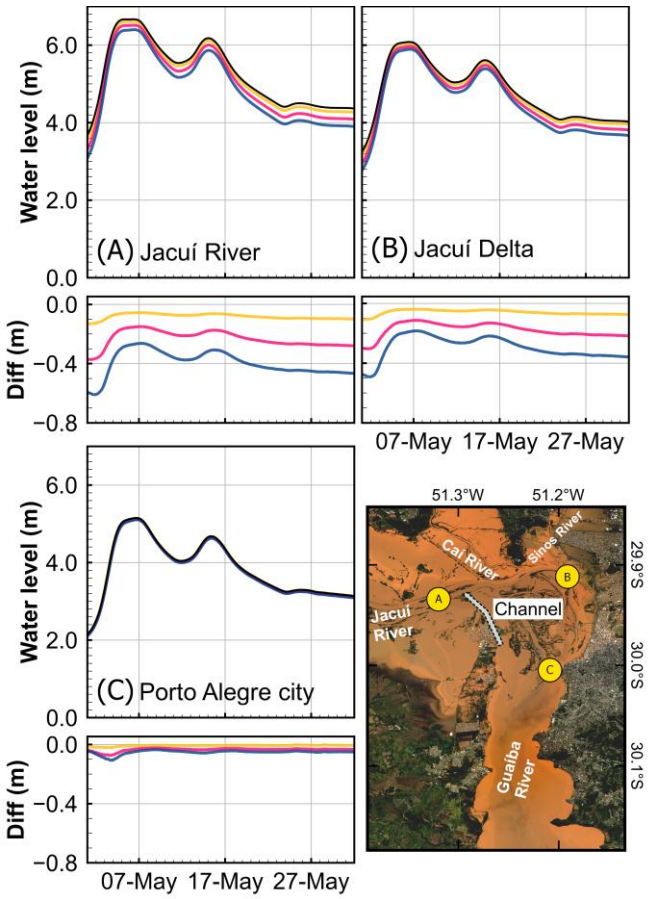

Figure ~~10~~11. Evaluated scenario for mitigating flooding in the RMPA involved a channel connecting the Jacuí and Guaíba ~~River~~rivers. Points A, B, and C illustrate the channel's effectiveness in reducing water levels around the Jacuí Delta.

~~2.2.6.~~4.3.2. Patos Lagoon channel

Formatted: Outline numbered + Level: 3 + Numbering Style: 1, 2, 3, … + Start at: 1 + Alignment: Left + Aligned at: 0 cm + Indent at: 0.63 cm

According to the model results (**Figure ~~11~~12**), the ~~connection~~ construction of a new channel ~~between~~ connecting the Patos Lago~~o~~on ~~and~~ to the Atlantic Ocean ~~by a new channel~~ could lower the average water levels ~~in the~~within the lagoon, while

having minimal impact on the maximum flow peak upstream in the Guaíba River. ~~The water levels at~~At the Point C (Cais Mauá station location), the maximum water level showed negligible change ~~indicated that the maximum flow peak remained unchanged~~, with reductions ~~a decreasing~~ of less than 0.10 meters ~~of the maximum water level in~~across all the simulated scenarios. ~~On the other hand~~Conversely, the results indicate a reduction in ~~it was noted a decrease of the~~ flood duration ~~by~~ of approximately ~~two~~2 days compared to the May flood event (**Figure ~~11a~~12a**).

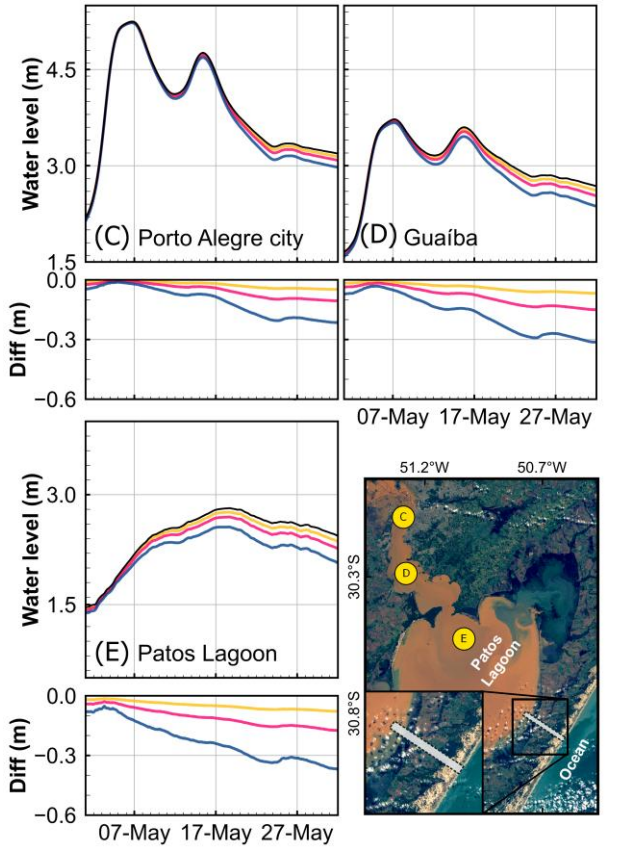

Figure 12. Second evaluated flood mitigation scenario for~~scenario for mitigating flooding in~~ the RMPA considered the construction of a channel connecting the Patos Lagoon and the Atlantic Ocean in th~~e~~its northeastern ~~part of the lagoon~~portion. Points C, D and E illustrate~~d~~ the influence~~d~~ of the channel ~~in~~on reducing flooding in the region.

Similar results were observed at Point D (**Figure ~~11b~~12b**) and Point E (**Figure ~~11c~~12c**), where the proposed hydraulic intervention ~~was~~ proved ~~not effective~~ineffective in reducing the water level peak, although it did ~~reduce~~ contribute to ~~the average water level and flood duration~~a slight decrease in average water levels and flood duration. At Point D, located in the ~~middle~~central-south~~ern~~ ~~part~~ reach of the Guaíba River, the reduction in the maximum peak was minimal (~~same as~~comparable to that observed at~~for~~ Point E). However, the ~~water levels showed~~simulations indicated maximum decreases of 0.07 meters for the 100-meter scenario, 0.15 meters for the 250-meter scenario, and 0.33 meters for the 500-meter scenario. At Point E, within the lagoon, ~~The~~the maximum reductions ranged from ~~decrease in water levels observed at Point E ranged from~~ 0.08 meters (100-meter scenario) to 0.39 meters (500-meter scenario)~~. in the lagoon.~~

~~Considering~~ Given that none of the three ~~scenarios demonstrated~~ evaluated scenarios produced significant changes in water levels across the ~~evaluated regions~~study area, the proposed structural measure appears ineffective for mitigating future flood events in the RMPA.~~we conclude that the proposed structural measure is ineffective in preventing further flood events in the RMPA.~~

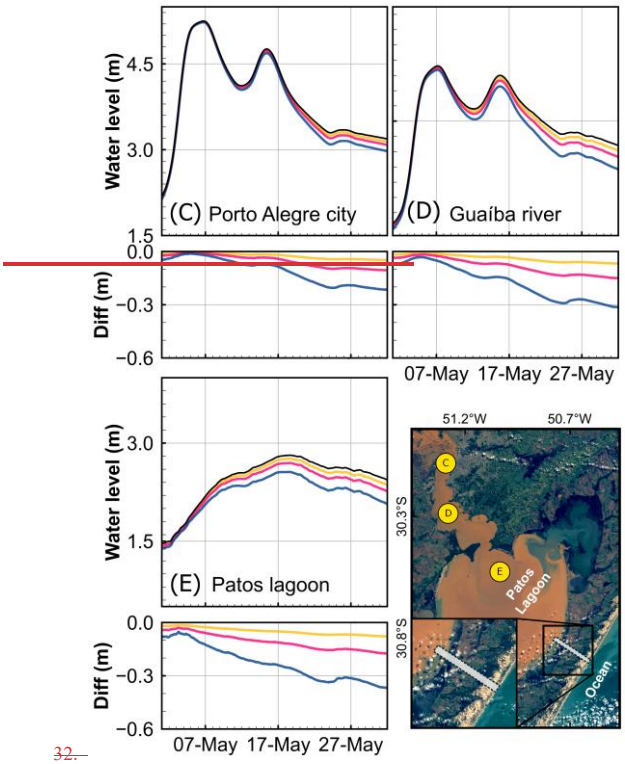

640 ~~32.~~

~~1.~~

~~5. Figure 11. Second evaluated scenario for mitigating flooding in the RMPA considered a channel connecting the Patos Lagoon and the Atlantic Ocean in the northeast part of the lagoon. Points C, D and E illustrated the influenced of the channel in reducing flood in the region.~~Discussion

645 **5.1. Model performance compared previous studies**

In this study, we calibrated and validated a two-dimensional hydrodynamic model using HEC-RAS software to simulate the extreme May 2024 flood event within the Patos Lagoon basin in southern Brazil. The model showed an overall robust performance, achieving an average RMSE of 0.71 meters, a NSE of 0.82 and a flood area reproduction rate of 83% on the validation dataset.

Formatted: Outline numbered + Level: 1 + Numbering Style: 1, 2, 3, … + Start at: 1 + Alignment: Left + Aligned at: 0 cm + Indent at: 0.63 cm

Formatted: Outline numbered + Level: 2 + Numbering Style: 1, 2, 3, … + Start at: 1 + Alignment: Left + Aligned at: 0 cm + Indent at: 0.63 cm

Regarding accuracy, the model exhibited an error of approximately -9% compared to the maximum water peak observed in the Guaíba River, and -23% over long-term water levels. This level of accuracy is relatively consistent with current studies employing 2D hydrodynamic models in moderate to large basins. Furthermore, the difference between minimum flood level and historic flood peaks in the basin is significantly higher than the average bias found. For instance, the historic floods of May 2024 (5.2 meters) and May 1941 (4.75 meters) are substantially higher than the minimum flood level of 3 meters (at Cais Mauá gauge station).

Our performance metrics are competitive with both regional and international studies utilizing similar modelling frameworks (Bhargav et al., 2025; Gomes Calixto et al., 2020; Shustikova et al., 2019). For instance, Shustikova et al (2019) reported an RMSE of 0.84 meters and a 77% flood-extent accuracy using a 100-meter subgrid mesh in HEC-RAS 2D to simulate a flood event in Italy. Similarly, Gomes et al (2021) employed HEC-RAS 2D in a northeastern Brazil and reported an 82% reproduction of the observed flood extent, which is comparable to the overall accuracy achieved in our study. Bhargav et al (2025) applied HEC-RAS to simulate floods in the lower portion of the Narmada Basin (<10,000 km²) in India, achieving an average NSE of 0.75 and an RMSE of 0.17 meters. Although their RMSE average is lower, it is important to note that our model represents an extreme flood event across a much larger system (~180,000 km²) influenced by multiple rivers inflows, highlighting the inherent challenges of hydrodynamic modelling in large basins and complex systems. Even given these conditions, we achieved RMSE values comparable to those for some of the rivers (see **Figure 5**).

Regarding studies focused on mitigation scenarios, the baseline accuracy of the proposed model is also consistent with those typically used for planning and policy evaluation (Gomes Calixto et al., 2020; Timbadiya et al., 2015). For instance, Timbadiya (2022) calibrated a 2D hydrodynamic model to evaluate the impact of proposed structures on flooding in the Narmada River, and obtained an RMSE of 0.84 meters and an NSE of 0.79. In the same context, Gomes Calixto et al. (2020) obtained an average NSE of 0.87 performance using a 2D model to assess flood-mitigation strategies in São Paulo.

~~was able to found effeitively flood control system for th~~

Formatted: Font: Bold

~~2.4.~~5.2. Uncertainties regarding the two-dimensional model

Formatted: Outline numbered + Level: 2 + Numbering Style: 1, 2, 3, … + Start at: 1 + Alignment: Left + Aligned at: 0 cm + Indent at: 0.63 cm

~~In this study we calibrated and validated a two-dimensional hydrodynamic model using HEC-RAS software to simulate the May 2024 flood in southern Brazil, Patos Lagoon basin.~~ There are some limitations regarding the model design for evaluating flooding in the study region. First, the results are depended on the DTM model data and bathymetry accuracy, which may reproduce flow propagation uncertainties due to DTM errors or limitations in its spatial resolution (30 meters). We used the ANADEM model, which demonstrates some accuracy improvements compared to other publicly available DEMs such as SRTM, COPDEM and FABDEM (Laipelt et al., 2024) for South America, with simulation results showing good agreement with observation data. Second, the upstream boundary conditions used in the model's design do not cover all the tributaries rivers of the study region due to lack of in-situ observations, which may lead to local underestimations. We expect that the

complete set up of independent sources validations adopted, including measured streamflow's, level gauges, satellite flooded areas and water slopes serves as quality control for models' system good representation and uncertainties understanding.

On the other hand, it is important to note that there are also uncertainties regarding the observation data used for validation. A report by Paiva et al. (2025) indicated uncertainties in the extrapolation of the rating curve, particularly in locations such as Rio Pardo on the Jacuí River and at points along the Taquari River, which are localities that contributed significantly to the flood formation. These uncertainties in the stage-discharge relationship for extreme flows may explain some of the localized differences observed between the simulated and observed water levels.

Formatted: Font color: Black

Formatted: Font color: Black

Among the flood mitigation scenarios, we additionally evaluated the sensitivity of the simulation for different parameters and proposed structures. Manning's roughness coefficient for the water bodies may influence the potential of the channels to mitigate flooding in the study region. Our sensitivity analysis showed that varying Manning's roughness coefficient in the Guaíba River between 0.025 to 0.045 would influence water flow peak in the Cais Mauá station (Point C) in -0.91 meters and 0.32 meters, respectively.

Furthermore, we utilized SWOT altimetry observations to verify the model's water level accuracy and to confirm water slope during the event, yielding results that aligned well with simulations. The application of SWOT mission data proved to be a valuable resource for acquiring information in areas with limited monitoring, enhancing our comprehension of flood dynamics and serving as supplementary data for validating hydrodynamic models.

~~2.5.~~5.3. Recommendations for flooding management strategies in the region

Formatted: Outline numbered + Level: 2 + Numbering Style: 1, 2, 3, … + Start at: 1 + Alignment: Left + Aligned at: 0 cm + Indent at: 0.63 cm

Measures to mitigate flooding impacts are urgent need for locations that are experiencing an increase in in extreme flood events due to climate change (Alfieri et al., 2016; Wang et al., 2022; Wasko et al., 2021), as is the case of southern Brazil. We assessed different flooding scenarios based on the unprecedented flood that devasted the RMPA in May 2024, focusing on its potential impact on densely populated areas.

The evaluation of river contributions and synchronized scenarios highlights the potential of hydrodynamic models for flood management, which has been demonstrated in many other studies(de Arruda Gomes et al., 2021; Bhargav et al., 2025; Gomes Calixto et al., 2020; Guse et al., 2020; Wulandari et al., 2025). Wulandari et al (2025) used HEC-RAS 2D to reproduce an extreme flood event in Indonesia and identified their Tallo River's main individual role int the event. Similarly, Guse et al (2020) analysed large German and Austrian river systems and evaluated the consequences of synchronized tributary rivers with the main river to floods.

Our results indicate that forecasting systems should prioritize accurate predictions of these Jacuí and Taquari rivers, including their timing relative to one another, as small changes in peak alignment can produce large impacts on the RMPA, in addition to the impact on cities alongside both rivers

Moreover, ~~O~~the~~ur~~ results regarding~~of~~ the hydraulic interventions showed that even the most effective configuration could only reduce peak flows by nearly 13% in the capital Porto Alegre, which is insufficient to prevent flooding in the affected areas. These findings suggest that the hydraulic interventions tested in this study would be of limited benefit in reducing the flooding due to the extreme rainfall in May 2024.

In this context, studies indicates that structural measures such as dike walls, levees may not be the most effective strategies for flood mitigation in the context of climate change (Alfieri et al., 2016; Burrell et al., 2007; Serra-Llobet et al., 2022), and in some scenarios could potentially increase flood hazard (Blöschl, 2022; Ommer et al., 2024). The implementation of protective structures also encourages development and investment in high-risk areas, potentially leading to more severe consequences when its failure, phenomenon kwon as the "levee effect" (Di Baldassarre et al., 2018). For instance, Porto Alegre's flood protection system, developed in the 1970s following historic floods in 1941 and 1967, the false sense of security encouraged increased urban development near these systems, which were the areas most affected during the May 2024 flood. The city Canoas, the second most populated city in the RMPA, experienced similar issues, with urbanization near its dike systems resulting in failures and a high number of houses being impacted by flooding (Collischonn et al., 2025).

To reduce the consequences of extreme flood events in the Patos Lagoon basin more non-structural interventions seems relevant. These included adopting zoning policies to limit development in flood-prone areas (Poussin et al., 2012; De Risi et al., 2015; Serra-Llobet et al., 2022). For example, spatial zoning measures in the Netherlands were found to have a risk reduction capacity of 25 to 45% (Poussin et al., 2012). Other important non-structural approaches include early warning systems, flood forecasting, and efforts to increase public awareness and improve behaviour responses to floods (Alfieri et al., 2012; Henriksen et al., 2018; Perera et al., 2020). Additionally, collaborative framework with public participation can also lead to more cost-efficient solutions to increase flood risk assessments across communities (Henriksen et al., 2018). The advantaged of non-structural measures included lower costs, greater sustainability, and easier of implementation (Dawson et al., 2011; Kundzewicz, 2002). Therefore, cities can mitigate flood risks by reducing population exposure to extreme floods without relying solely on structural solutions (Hall et al., 2006; Majidi et al., 2019), due to their complexity and high maintained costs, and often only minimalize impacts, and are challenging to adapt to climate change scenarios (Burrell et al., 2007; Serra-Llobet et al., 2022).

6. Conclusion

~~## 2. Conclusion~~

Our study evaluated different flood scenarios in southern Brazil's RMPA region, based on historical ~~flood~~ May 2024 flood. The analysis ~~was based using~~was conducted using 2D hydrodynamic modelling, which was validated using water level, flood extent and streamflow data, demonstrating accurate representation of the May 2024 event.

Our findings ~~address the following scientific questions~~are summarized as follow:

Formatted: Outline numbered + Level: 3 + Numbering Style: 1, 2, 3, … + Start at: 1 + Alignment: Left + Aligned at: 0 cm + Indent at: 0.63 cm

Formatted: Outline numbered + Level: 1 + Numbering Style: 1, 2, 3, … + Start at: 1 + Alignment: Left + Aligned at: 0 cm + Indent at: 0.63 cm

(i) The Taquari River was responsible for most of the flow peaks in the RMPA, while the Jacuí River contributed to the flood's duration. Others (Caí, Sinos and Gravataí) flowing into the Guaíba River did not significantly impact overall water levels in the RMPA, although contributed to localized flooding.

(ii) Synchronized flow peaks of the Jacuí and Taquari Rivers in the Guaíba River would have increased water levels by 0.82 meters, exacerbating the flood scenario in the RMPA. At the Cais Mauá station, water levels would have exceeded 6 meters, surpassing the threshold for the flood protection system developed for the city of Porto Alegre. This scenario, constructed using May 2024 flood conditions but advancing the Jacuí River's flow peak by approximately 4 days, presents a significant risk to the state capital and remains plausible under heavy rainfall conditions common in the region.

(iii) The proposed hydraulic structures of additional channels alternatives would not have been sufficient to prevent RMPA flooding entirely. Our results also indicated that the degree of flood mitigation structures would not have been uniform across the RMPA. This spatial disparity in performance suggests that the limited overall impact may be linked to a combination of factors, including the specific design of the interventions, local hydrogeomorphic features, and the unprecedented magnitude of the flood event itself~~suggested that the reduction in flooding would depend on location, despite having minimum effectiveness for the cities surrounding the severely affected RMPA~~.

~~We want to highlight the delimitations of these experiments, which only consider hydraulic impacts within the Patos Lagoon basin. Implementing interventions in the natural hydrodynamic system must account for factors such as engineering availability, implementation costs, and maintenance expenses. Additionally, these hydrodynamic alterations could negatively impact the environment, potentially causing erosion, navigation issues, reduced agriculture productivity and salinization, particularly in the case of an open channel connecting the Patos Lagoon to the ocean.~~

The analyses reported in this study can aid decision-makers in improving flood management strategies for RMPA region, emphasizing the vital role of hydrodynamic models in predicting and evaluating hydraulic interventions, as well as identifying opportunities for non-structural measures. Future research should benefit of high-resolution (1 to 5 meters) data based on Light Detection and Ranging (LiDAR) sensors to assess the impact of urbanization on regional flooding and identify risk zones in the context of increased flooding due to climate change.

Finally, this research advances a methodological framework predicated on multi-source data integration for the robust performance assessment of hydrodynamic simulations. By incorporating multiple, independent observational datasets, we significantly enhanced the model's predictive accuracy and its fidelity in reproducing this flood event~~Finally, f~~. ~~rom a broader worldwide perspective,~~ We expect that the presented methods will serve as a reference for studies in other locations, as well as for analyses of the efficiency of structural measures for flood control.~~we expected that the presented methods would serve as a framework benchmark for other locations studies regarding climate change and floods adaptation, and that our results can serve as example for structural and non-structural measures selection and evaluation.~~

Data availability

The water level data used in this study are provided by the Brazilian Water Agency and Sanitation (ANA) (https://www.snirh.gov.br/hidrotelemetria/, accessed in July, 2024). The tidal data is available at the SIMCosta platform (https://simcosta.furg.br/home, accessed in August, 2024). The meteorological data are available at (https://bdmep.inmet.gov.br/, accessed in August, 2024) by the National Meteorological Institute of Brazil (INMET). SWOT data can be accessed through the NASA Earth Data repository (https://search.earthdata.nasa.gov/search, accessed in June, 2024). The digital terrain model (DTM) is publicly available on Google Earth Engine platform.

Author contributions

LL, FMF and RCDP contributed to the study's conception and design. LL and FMF wrote the manuscript draft. LL performed model simulations analysed the data. RCDP, MS, WC~~, EETJ~~ and AR reviewed and edited the manuscript.

Competing interests

The author declares that there is no conflict of interest.

Acknowledgement

The authors would like to gratefully acknowledge the support of the Google Earth Engine team. We thank the Brazilian National Water and Sanitation Agency (ANA) and the Geological Service of Brazil (SGB) for their efforts in providing high-quality in-situ observations during the 2024 floods. We also thank~~s~~ CNES and NASA for making SWOT mission data publicly available. We also thank the reviewers for their valuable contribution for the final version of the manuscript.

Financial support

This research has been supported by the Brazilian National Council for Scientific and Technological Development (CNPq).

References

Abdella, K. and Mekuanent, F.: Application of hydrodynamic models for designing structural measures for river flood mitigation: the case of Kulfo River in southern Ethiopia, Model Earth Syst Environ, 7, 2779–2791, https://doi.org/10.1007/s40808-020-01057-5, 2021.

AIRBUS: Copernicus DEM: Copernicus digital elevation model product handbook, Report AO/1-9422/18/IL G, 2020.

Alfieri, L., Salamon, P., Pappenberger, F., Wetterhall, F., and Thielen, J.: Operational early warning systems for water-related hazards in Europe, Environ Sci Policy, 21, 35–49, https://doi.org/https://doi.org/10.1016/j.envsci.2012.01.008, 2012.

Alfieri, L., Feyen, L., and Di Baldassarre, G.: Increasing flood risk under climate change: a pan-European assessment of the benefits of four adaptation strategies, Clim Change, 136, 507–521, https://doi.org/10.1007/s10584-016-1641-1, 2016.

Alves, M. E. P., Fan, F. M., Paiva, R. C. D. de, Siqueira, V. A., Fleischmann, A. S., Brêda, J. P., Laipelt, L., and Araújo, A. A.: Assessing the capacity of large-scale hydrologic-hydrodynamic models for mapping flood hazard in southern Brazil, RBRH, 27, 2022.

Andrade, M. M., Piazera, M., Luz, R. da, Nunes, J. C. R., Scottá, F., and Silva, T.: Flow measurements with ADCP on the Guaíba River, during the highest water level recorded in history - May 2024 (floods in the State of Rio Grande do Sul, Brazil), RBRH, 29, 2024.

António, M. H. P., Fernandes, E. H., and Muelbert, J. H.: Impact of Jetty Configuration Changes on the Hydrodynamics of the Subtropical Patos Lagoon Estuary, Brazil, Water (Basel), 12, https://doi.org/10.3390/w12113197, 2020.

de Arruda Gomes, M. M., de Melo Verçosa, L. F., and Cirilo, J. A.: Hydrologic models coupled with 2D hydrodynamic model for high-resolution urban flood simulation, Natural Hazards, 108, 3121–3157, https://doi.org/10.1007/s11069-021-04817-3, 2021.

Ávila, A., Justino, F., Wilson, A., Bromwich, D., and Amorim, M.: Recent precipitation trends, flash floods and landslides in southern Brazil, Environmental Research Letters, 11, 114029, https://doi.org/10.1088/1748-9326/11/11/114029, 2016.

Di Baldassarre, G., Kreibich, H., Vorogushyn, S., Aerts, J., Arnbjerg-Nielsen, K., Barendrecht, M., Bates, P., Borga, M., Botzen, W., Bubeck, P., De Marchi, B., Llasat, C., Mazzoleni, M., Molinari, D., Mondino, E., Mård, J., Petrucci, O., Scolobig, A., Viglione, A., and Ward, P. J.: Hess Opinions: An interdisciplinary research agenda to explore the unintended consequences of structural flood protection, Hydrol Earth Syst Sci, 22, 5629–5637, https://doi.org/10.5194/hess-22-5629-2018, 2018.

Bartiko, D., Oliveira, D. Y., Bonumá, N. B., and Chaffe, P. L. B.: Spatial and seasonal patterns of flood change across Brazil, Hydrological Sciences Journal, 64, 1071–1079, https://doi.org/10.1080/02626667.2019.1619081, 2019.

Bates, P. D. and De Roo, A. P. J.: A simple raster-based model for flood inundation simulation, J Hydrol (Amst), 236, 54–77, https://doi.org/https://doi.org/10.1016/S0022-1694(00)00278-X, 2000.

Bates, P. D., Marks, K. J., and Horritt, M. S.: Optimal use of high-resolution topographic data in flood inundation models, Hydrol Process, 17, 537–557, https://doi.org/https://doi.org/10.1002/hyp.1113, 2003.

Bhargav, A. M., Suresh, R., Tiwari, M. K., Trambadia, N. K., Chandra, R., and Nirala, S. K.: Development of a 2D hydrodynamic model for flood assessment for the lower Narmada basin, Gujarat (India), Journal of Water and Climate Change, 16, 1567–1585, https://doi.org/10.2166/wcc.2025.706, 2025.

Biancamaria, S., Lettenmaier, D. P., and Pavelsky, T. M.: The SWOT Mission and Its Capabilities for Land Hydrology, Surv Geophys, 37, 307–337, https://doi.org/10.1007/s10712-015-9346-y, 2016.

Blöschl, G.: Three hypotheses on changing river flood hazards, Hydrol Earth Syst Sci, 26, 5015–5033, https://doi.org/10.5194/hess-26-5015-2022, 2022.

Brêda, J. P. L. F., Cauduro Dias de Paiva, R., Siqueira, V. A., and Collischonn, W.: Assessing climate change impact on flood discharge in South America and the influence of its main drivers, J Hydrol (Amst), 619, 129284, https://doi.org/https://doi.org/10.1016/j.jhydrol.2023.129284, 2023.

Burrell, B. C., Davar, K., and Hughes, R.: A Review of Flood Management Considering the Impacts of Climate Change, Water Int, 32, 342–359, https://doi.org/10.1080/02508060708692215, 2007.

Cai, T., Li, X., Ding, X., Wang, J., and Zhan, J.: Flood risk assessment based on hydrodynamic model and fuzzy comprehensive evaluation with GIS technique, International Journal of Disaster Risk Reduction, 35, 101077, https://doi.org/https://doi.org/10.1016/j.ijdrr.2019.101077, 2019.

Cavalcante, M. R. G., da Cunha Luz Barcellos, P., and Cataldi, M.: Flash flood in the mountainous region of Rio de Janeiro state (Brazil) in 2011: part I—calibration watershed through hydrological SMAP model, Natural Hazards, 102, 1117–1134, https://doi.org/10.1007/s11069-020-03948-3, 2020.

Chagas, V. B. P., Chaffe, P. L. B., and Blöschl, G.: Climate and land management accelerate the Brazilian water cycle, Nat Commun, 13, 5136, https://doi.org/10.1038/s41467-022-32580-x, 2022.

Chow, V. Te: Open-channel Hydraulics, McGraw-Hill, 1959.

Collischonn, W., Ruhoff, A., Filho Cabeleira, R., Paiva, R., Fan, F., and Possa, T.: Chuva da cheia de 2024 foi mais volumosa e intensa que a da cheia de 1941 na bacia hidrográfica do Guaíba, Porto Alegre, 1–8 pp., 2024.

Collischonn, W., Fan, F. M., Possantti, I., Dornelles, F., Paiva, R., Sampaio, M., Michel, G., Magalhães Filho, F. J. C., Moraes, S. R., Marcuzzo, F. F. N., Michel, R. D. L. M., Beskow, T. L. C., Beskow, S., Fernandes, E., Laipelt, L., Ruhoff, A., Kobiyana, M., Collares, L. G., Buffon, F., Duarte, E., Lima, S., Meirelles, F. S. C., and Allasia, D.: The exceptional hydrological disaster of April-May 2024 in southern Brazil, Revista Brasileira de Recursos Hídricos, 1, https://doi.org/10.1590/2318-0331.302520240119, 2025.

Damião Mendes, M. C. and Cavalcanti, I. F. A.: The relationship between the Antarctic oscillation and blocking events over the South Pacific and Atlantic Oceans, International Journal of Climatology, 34, 529–544, https://doi.org/https://doi.org/10.1002/joc.3729, 2014.

Dawson, R. J., Ball, T., Werritty, J., Werritty, A., Hall, J. W., and Roche, N.: Assessing the effectiveness of non-structural flood management measures in the Thames Estuary under conditions of socio-economic and environmental change, Global Environmental Change, 21, 628–646, https://doi.org/https://doi.org/10.1016/j.gloenvcha.2011.01.013, 2011.

DRRS: Programa do Governo Holandês de Redução de Risco de Desastres e Suportes a Surtos (DRRS). Final Report., 2024.

Durand, M., Fu, L.-L., Lettenmaier, D. P., Alsdorf, D. E., Rodriguez, E., and Esteban-Fernandez, D.: The Surface Water and Ocean Topography Mission: Observing Terrestrial Surface Water and Oceanic Submesoscale Eddies, Proceedings of the IEEE, 98, 766–779, https://doi.org/10.1109/JPROC.2010.2043031, 2010.

Dutta, D., Alam, J., Umeda, K., Hayashi, M., and Hironaka, S.: A two-dimensional hydrodynamic model for flood inundation simulation: a case study in the lower Mekong river basin, Hydrol Process, 21, 1223–1237, https://doi.org/https://doi.org/10.1002/hyp.6682, 2007.

Fernandes, E., Dyer, K. R., and Niencheski, L. F.: TELEMAC-2D calibration and validation to the hydrodynamics of the Patos Lagoon (Brazil), J Coast Res, 34, 470–488, 2001.

Fernandes, E. H. L., Dyer, K. R., Moller, O. O., and Niencheski, L. F. H.: The Patos Lagoon hydrodynamics during an El Niño event (1998), Cont Shelf Res, 22, 1699–1713, https://doi.org/https://doi.org/10.1016/S0278-4343(02)00033-X, 2002.

Fewtrell, T. J., Duncan, A., Sampson, C. C., Neal, J. C., and Bates, P. D.: Benchmarking urban flood models of varying complexity and scale using high resolution terrestrial LiDAR data, Physics and Chemistry of the Earth, Parts A/B/C, 36, 281–291, https://doi.org/https://doi.org/10.1016/j.pce.2010.12.011, 2011.

Fleischmann, A., Paiva, R., and Collischonn, W.: Can regional to continental river hydrodynamic models be locally relevant? A cross-scale comparison, J Hydrol X, 3, 100027, https://doi.org/https://doi.org/10.1016/j.hydroa.2019.100027, 2019.

François, F. S.: Modelagem hidrodinâmica de áreas suscetíveis a inundação no município de nova Santa Rita (RS), Trabalho de Conclusão de curso, Universidade Federal do Rio Grande do Sul, Porto Alegre, 2021.

Fu, L.-L., Pavelsky, T., Cretaux, J.-F., Morrow, R., Farrar, J. T., Vaze, P., Sengenes, P., Vinogradova-Shiffer, N., Sylvestre-Baron, A., Picot, N., and Dibarboure, G.: The Surface Water and Ocean Topography Mission: A Breakthrough in Radar Remote Sensing of the Ocean and Land Surface Water, Geophys Res Lett, 51, e2023GL107652, https://doi.org/https://doi.org/10.1029/2023GL107652, 2024.

GEBCO: GEBCO 2024 Grid, https://doi.org/doi:10.5285/1c44ce99-0a0d-5f4f-e063-7086abc0ea0f, 2024.

Ghanbarpour, M. R., Salimi, S., and Hipel, K. W.: A comparative evaluation of flood mitigation alternatives using GIS-based river hydraulics modelling and multicriteria decision analysis, J Flood Risk Manag, 6, 319–331, https://doi.org/https://doi.org/10.1111/jfr3.12017, 2013.

Gomes Calixto, K., Wendland, E. C., and Melo, D. de C. D.: Hydrologic performance assessment of regulated and alternative strategies for flood mitigation: a case study in São Paulo, Brazil, Urban Water J, 17, 481–489, https://doi.org/10.1080/1573062X.2020.1773509, 2020.

Guse, B., Merz, B., Wietzke, L., Ullrich, S., Viglione, A., and Vorogushyn, S.: The role of flood wave superposition in the severity of large floods, Hydrol Earth Syst Sci, 24, 1633–1648, https://doi.org/10.5194/hess-24-1633-2020, 2020.

Hall, J. W., Sayers, P. B., Walkden, M. J. A., and Panzeri, M.: Impacts of climate change on coastal flood risk in England and Wales: 2030–2100, Philosophical Transactions of the Royal Society A: Mathematical, Physical and Engineering Sciences, 364, 1027–1049, https://doi.org/10.1098/rsta.2006.1752, 2006.

Hammond, J. C., Anderson, B., Simeone, C., Brunner, M., Munoz-Castro, E., Archfield, S., Magee, E., and Armitage, R.: Hydrological whiplash: Highlighting the need for better understanding and quantification of sub-seasonal hydrological extreme transitions, Hydrol Process, 39, https://doi.org/10.1002/hyp.70113, 2025.

Heinrich, P., Hagemann, S., Weisse, R., Schrum, C., Daewel, U., and Gaslikova, L.: Compound flood events: analysing the joint occurrence of extreme river discharge events and storm surges in northern and central Europe, Natural Hazards and Earth System Sciences, 23, 1967–1985, https://doi.org/10.5194/nhess-23-1967-2023, 2023.

Hendry, A., Haigh, I. D., Nicholls, R. J., Winter, H., Neal, R., Wahl, T., Joly-Laugel, A., and Darby, S. E.: Assessing the characteristics and drivers of compound flooding events around the UK coast, Hydrol Earth Syst Sci, 23, 3117–3139, https://doi.org/10.5194/hess-23-3117-2019, 2019.

Henriksen, H. J., Roberts, M. J., van der Keur, P., Harjanne, A., Egilson, D., and Alfonso, L.: Participatory early warning and monitoring systems: A Nordic framework for web-based flood risk management, International Journal of Disaster Risk Reduction, 31, 1295–1306, https://doi.org/https://doi.org/10.1016/j.ijdrr.2018.01.038, 2018.

Hillman, G., Rodriguez, A., Pagot, M., Tyrrell, D., Corral, M., Oroná, C., and Möller, O.: 2D Numerical Simulation of Mangueira Bay Hydrodynamics, J Coast Res, 2010, 108–115, https://doi.org/10.2112/1551-5036-47.sp1.108, 2007.

Hsu, S. A.: Coastal Meteorology, in: Encyclopedia of Physical Science and Technology, Elsevier, 155–173, https://doi.org/10.1016/B0-12-227410-5/00114-9, 2003.

Hunt, J. D., Silva, C. V., Fonseca, E., de Freitas, M. A. V., Brandão, R., and Wada, Y.: Role of pumped hydro storage plants for flood control, J Energy Storage, 104, 114496, https://doi.org/https://doi.org/10.1016/j.est.2024.114496, 2024.

Kjerfve, B.: COMPARATIVE OCEANOGRAPHY OF COASTAL LAGOONS, in: Estuarine Variability, edited by: Wolfe, D. A., Elsevier, 63–81, https://doi.org/10.1016/B978-0-12-761890-6.50009-5, 1986.

Kundzewicz, Z. W.: Non-structural Flood Protection and Sustainability, Water Int, 27, 3–13, https://doi.org/10.1080/02508060208686972, 2002.

Laipelt, L., de Andrade, B., Collischonn, W., de Amorim Teixeira, A., Paiva, R. C. D. de, and Ruhoff, A.: ANADEM: A Digital Terrain Model for South America, Remote Sens (Basel), 16, https://doi.org/10.3390/rs16132321, 2024.

Laipelt, L., de Paiva, R. C. D., Fan, F. M., Collischonn, W., Papa, F., and Ruhoff, A.: SWOT Reveals How the 2024 Disastrous Flood in South Brazil Was Intensified by Increased Water Slope and Wind Forcing, Geophys Res Lett, 52, e2024GL111287, https://doi.org/https://doi.org/10.1029/2024GL111287, 2025.

Leonard, M., Westra, S., Phatak, A., Lambert, M., van den Hurk, B., McInnes, K., Risbey, J., Schuster, S., Jakob, D., and Stafford-Smith, M.: A compound event framework for understanding extreme impacts, WIREs Climate Change, 5, 113–128, https://doi.org/https://doi.org/10.1002/wcc.252, 2014.

Lesser, G. R., Roelvink, J. A. v, van Kester, J. A. T. M., and Stelling, G. S.: Development and validation of a three-dimensional morphological model, Coastal engineering, 51, 883–915, 2004.

Li, W., Lin, K., Zhao, T., Lan, T., Chen, X., Du, H., and Chen, H.: Risk assessment and sensitivity analysis of flash floods in ungauged basins using coupled hydrologic and hydrodynamic models, J Hydrol (Amst), 572, 108–120, https://doi.org/https://doi.org/10.1016/j.jhydrol.2019.03.002, 2019.

Lima, R. C. de A. and Barbosa, A. V. B.: Natural disasters, economic growth and spatial spillovers: Evidence from a flash flood in Brazil, Papers in Regional Science, 98, 905–925, https://doi.org/https://doi.org/10.1111/pirs.12380, 2019.

Majidi, A. N., Vojinovic, Z., Alves, A., Weesakul, S., Sanchez, A., Boogaard, F., and Kluck, J.: Planning Nature-Based Solutions for Urban Flood Reduction and Thermal Comfort Enhancement, Sustainability, 11, https://doi.org/10.3390/su11226361, 2019.

Marengo, J. A., Alcantara, E., Cunha, A. P., Seluchi, M., Nobre, C. A., Dolif, G., Goncalves, D., Assis Dias, M., Cuartas, L. A., Bender, F., Ramos, A. M., Mantovani, J. R., Alvalá, R. C., and Moraes, O. L.: Flash floods and landslides in the city of

Recife, Northeast Brazil after heavy rain on May 25–28, 2022: Causes, impacts, and disaster preparedness, Weather Clim Extrem, 39, 100545, https://doi.org/https://doi.org/10.1016/j.wace.2022.100545, 2023.

Marks, K. and Bates, P.: Integration of high-resolution topographic data with floodplain flow models, Hydrol Process, 14, 2109–2122, https://doi.org/https://doi.org/10.1002/1099-1085(20000815/30)14:11/12<2109::AID-HYP58>3.0.CO;2-1, 2000.

Marques, W. C., Fernandes, E. H., Monteiro, I. O., and Möller, O. O.: Numerical modeling of the Patos Lagoon coastal plume, Brazil, Cont Shelf Res, 29, 556–571, https://doi.org/https://doi.org/10.1016/j.csr.2008.09.022, 2009.

Martins, F. and Fernandes, E.: HYDRODYNAMIC MODEL INTERCOMPARISON FOR THE PATOS LAGOON (BRAZIL), 2004.

Masood, M. and Takeuchi, K.: Assessment of flood hazard, vulnerability and risk of mid-eastern Dhaka using DEM and 1D hydrodynamic model, Natural Hazards, 61, 757–770, https://doi.org/10.1007/s11069-011-0060-x, 2012.

McMillan, H. K., Westerberg, I. K., and Krueger, T.: Hydrological data uncertainty and its implications, WIREs Water, 5, e1319, https://doi.org/https://doi.org/10.1002/wat2.1319, 2018.

Ming, X., Liang, Q., Xia, X., Li, D., and Fowler, H. J.: Real-Time Flood Forecasting Based on a High-Performance 2-D Hydrodynamic Model and Numerical Weather Predictions, Water Resour Res, 56, e2019WR025583, https://doi.org/https://doi.org/10.1029/2019WR025583, 2020.

Möller, O. O., Lorenzzentti, J. A., Stech, JoséL., and Mata, M. M.: The Patos Lagoon summertime circulation and dynamics, Cont Shelf Res, 16, 335–351, https://doi.org/10.1016/0278-4343(95)00014-R, 1996.

Neal, J., Schumann, G., Fewtrell, T., Budimir, M., Bates, P., and Mason, D.: Evaluating a new LISFLOOD-FP formulation with data from the summer 2007 floods in Tewkesbury, UK, J Flood Risk Manag, 4, 88–95, https://doi.org/https://doi.org/10.1111/j.1753-318X.2011.01093.x, 2011.

O'Loughlin, F. E., Neal, J., Schumann, G. J. P., Beighley, E., and Bates, P. D.: A LISFLOOD-FP hydraulic model of the middle reach of the Congo, J Hydrol (Amst), 580, 124203, https://doi.org/https://doi.org/10.1016/j.jhydrol.2019.124203, 2020.

Ommer, J., Neumann, J., Kalas, M., Blackburn, S., and Cloke, H. L.: Surprise floods: the role of our imagination in preparing for disasters, Natural Hazards and Earth System Sciences, 24, 2633–2646, https://doi.org/10.5194/nhess-24-2633-2024, 2024.

Paiva, R. C. D., Collischonn, W., and Buarque, D. C.: Validation of a full hydrodynamic model for large-scale hydrologic modelling in the Amazon, Hydrol Process, 27, 333–346, https://doi.org/https://doi.org/10.1002/hyp.8425, 2013.

Paiva, R. C. dias de, Mainardi Fan, F., Collischonn, W., Sampaio, M., Cristina de Oliveira, R., Lima, S., Camargo, P., and Massochin Medeiros, P.: Caracterização e modelagem das cheias de 2023 e 2024 no Rio Grande do Sul em escala regional. Relatório Técnico., 2025.

Patel, D. P., Ramirez, J. A., Srivastava, P. K., Bray, M., and Han, D.: Assessment of flood inundation mapping of Surat city by coupled 1D/2D hydrodynamic modeling: a case application of the new HEC-RAS 5, Natural Hazards, 89, 93–130, https://doi.org/10.1007/s11069-017-2956-6, 2017.

Perera, D., Agnihotri, J., Seidou, O., and Djalante, R.: Identifying societal challenges in flood early warning systems, International Journal of Disaster Risk Reduction, 51, 101794, https://doi.org/https://doi.org/10.1016/j.ijdrr.2020.101794, 2020.

Planet Team: Planet Application Program Interface: In Space for Life on Earth. San Francisco, CA , https://api.planet.com/, 2024.

Possa, T. M., Collischonn, W., Jardim, P. F., and Fan, F. M.: Hydrological-hydrodynamic simulation and analysis of the possible influence of the wind in the extraordinary flood of 1941 in Porto Alegre, RBRH, 27, e29, https://doi.org/10.1590/2318-0331.272220220028, 2022.

Poussin, J. K., Bubeck, P., Aerts, J. C. J. H., and Ward, P. J.: Potential of semi-structural and non-structural adaptation strategies to reduce future flood risk: case study for the Meuse, Natural Hazards and Earth System Sciences, 12, 3455–3471, https://doi.org/10.5194/nhess-12-3455-2012, 2012.

De Risi, R., Jalayer, F., and De Paola, F.: Meso-scale hazard zoning of potentially flood prone areas, J Hydrol (Amst), 527, 316–325, https://doi.org/https://doi.org/10.1016/j.jhydrol.2015.04.070, 2015.

Seiler, L. M. N., Fernandes, E. H. L., and Siegle, E.: Effect of wind and river discharge on water quality indicators of a coastal lagoon, Reg Stud Mar Sci, 40, 101513, https://doi.org/https://doi.org/10.1016/j.rsma.2020.101513, 2020.

Serra-Llobet, A., Jähnig, S. C., Geist, J., Kondolf, G. M., Damm, C., Scholz, M., Lund, J., Opperman, J. J., Yarnell, S. M., Pawley, A., Shader, E., Cain, J., Zingraff-Hamed, A., Grantham, T. E., Eisenstein, W., and Schmitt, R.: Restoring Rivers and Floodplains for Habitat and Flood Risk Reduction: Experiences in Multi-Benefit Floodplain Management From California and Germany, Front Environ Sci, 9, https://doi.org/10.3389/fenvs.2021.778568, 2022.

Shustikova, I., Domeneghetti, A., Neal, J. C., Bates, P., and Castellarin, A.: Comparing 2D capabilities of HEC-RAS and LISFLOOD-FP on complex topography, Hydrological Sciences Journal, 64, 1769–1782, https://doi.org/10.1080/02626667.2019.1671982, 2019.

Silva, R. A. G., Reis, R. C. S., Ramos, D. M., Belém, A. L., Puhl, E., and Manica, R.: Análise de Abertura de Novo Canal de Maré na Lagoa dos Patos para Atenuação de Cheias no Rio Guaíba, RS, in: II FLUHIDROS - Simpósio Nacional de Mecânica dos Fluidos e Hidráulica e XVI ENES - Encontro Nacional de Engenharia de Sedimentos, 2024a.

Silva, T. S., Toldo Jr., E. E., Nunes, J. C. R., Castro, N., Funke, N., Nievinski, F., Manica, R., Puhl, E., Fick, C., Scottá, F., Silva, M. L. R., and Ävila, I. M.: Nota Técnica - Vazões no Rio Guaíba durante os picos da enchente de maio de 2024, 1–2 pp., 2024b.

Stevenson, S., Coats, S., Touma, D., Cole, J., Lehner, F., Fasullo, J., and Otto-Bliesner, B.: Twenty-first century hydroclimate: A continually changing baseline, with more frequent extremes, Proceedings of the National Academy of Sciences, 119, e2108124119, https://doi.org/10.1073/pnas.2108124119, 2022.

Swain, D. L., Prein, A. F., Abatzoglou, J. T., Albano, C. M., Brunner, M., Diffenbaugh, N. S., Singh, D., Skinner, C. B., and Touma, D.: Hydroclimate volatility on a warming Earth, Nat Rev Earth Environ, 6, 35–50, https://doi.org/10.1038/s43017-024-00624-z, 2025.

Timbadiya, P. V, Patel, P. L., and Porey, P. D.: A 1D–2D Coupled Hydrodynamic Model for River Flood Prediction in a Coastal Urban Floodplain, J Hydrol Eng, 20, 05014017, https://doi.org/10.1061/(ASCE)HE.1943-5584.0001029, 2015.

USACE: HEC-RAS river analysis system hydraulic reference manual. Version 5.0, 2016.

Wang, T., Lu, Y., Liu, T., Zhang, Y., Yan, X., and Liu, Y.: The determinants affecting the intention of urban residents to prepare for flood risk in China, Natural Hazards and Earth System Sciences, 22, 2185–2199, https://doi.org/10.5194/nhess-22-2185-2022, 2022.

Wasko, C., Nathan, R., Stein, L., and O'Shea, D.: Evidence of shorter more extreme rainfalls and increased flood variability under climate change, J Hydrol (Amst), 603, 126994, https://doi.org/https://doi.org/10.1016/j.jhydrol.2021.126994, 2021.

Wulandari, S., Pratama, F., Andika, N., Wongso, P., Wijayasari, W., and Rohmat, F. I. W.: Identifying dominant river contributions to urban flooding: a scenario-based study of Makassar City, Front Built Environ, Volume 11-2025, 2025.

Zarzuelo, C., Díez-Minguito, M., Ortega-Sánchez, M., López-Ruiz, A., and Losada, M. Á.: Hydrodynamics response to planned human interventions in a highly altered embayment: The example of the Bay of Cádiz (Spain), Estuar Coast Shelf Sci, 167, 75–85, https://doi.org/https://doi.org/10.1016/j.ecss.2015.07.010, 2015.

Zhang, H., Wu, W., Hu, C., Hu, C., Li, M., Hao, X., and Liu, S.: A distributed hydrodynamic model for urban storm flood risk assessment, J Hydrol (Amst), 600, 126513, https://doi.org/https://doi.org/10.1016/j.jhydrol.2021.126513, 2021.

~~Abdella, K. and Mekuanent, F.: Application of hydrodynamic models for designing structural measures for river flood mitigation: the case of Kulfo River in southern Ethiopia, Model Earth Syst Environ, 7, 2779–2791, https://doi.org/10.1007/s40808-020-01057-5, 2021.~~

~~AIRBUS: Copernicus DEM: Copernicus digital elevation model product handbook, Report AO/1-9422/18/IL G, 2020.~~

~~Alfieri, L., Salamon, P., Pappenberger, F., Wetterhall, F., and Thielen, J.: Operational early warning systems for water-related hazards in Europe, Environ Sci Policy, 21, 35–49, https://doi.org/https://doi.org/10.1016/j.envsci.2012.01.008, 2012.~~

~~Alfieri, L., Feyen, L., and Di Baldassarre, G.: Increasing flood risk under climate change: a pan-European assessment of the benefits of four adaptation strategies, Clim Change, 136, 507–521, https://doi.org/10.1007/s10584-016-1641-1, 2016.~~

~~Alves, M. E. P., Fan, F. M., Paiva, R. C. D. de, Siqueira, V. A., Fleischmann, A. S., Brêda, J. P., Laipelt, L., and Araújo, A. A.: Assessing the capacity of large-scale hydrologic-hydrodynamic models for mapping flood hazard in southern Brazil, RBRH, 27, 2022.~~

~~Andrade, M. M., Piazera, M., Luz, R. da, Nunes, J. C. R., Scottá, F., and Silva, T.: Flow measurements with ADCP on the Guaíba River, during the highest water level recorded in history - May 2024 (floods in the State of Rio Grande do Sul, Brazil), RBRH, 29, 2024.~~

~~António, M. H. P., Fernandes, E. H., and Muelbert, J. H.: Impact of Jetty Configuration Changes on the Hydrodynamics of the Subtropical Patos Lagoon Estuary, Brazil, Water (Basel), 12, https://doi.org/10.3390/w12113197, 2020.~~

~~de Arruda Gomes, M. M., de Melo Verçosa, L. F., and Cirilo, J. A.: Hydrologic models coupled with 2D hydrodynamic model for high-resolution urban flood simulation, Natural Hazards, 108, 3121–3157, https://doi.org/10.1007/s11069-021-04817-3, 2021.~~

~~Ávila, A., Justino, F., Wilson, A., Bromwich, D., and Amorim, M.: Recent precipitation trends, flash floods and landslides in southern Brazil, Environmental Research Letters, 11, 114029, https://doi.org/10.1088/1748-9326/11/11/114029, 2016.~~

Di Baldassarre, G., Kreibich, H., Vorogushyn, S., Aerts, J., Arnbjerg-Nielsen, K., Barendrecht, M., Bates, P., Borga, M., Botzen, W., Bubeck, P., De Marchi, B., Llasat, C., Mazzoleni, M., Molinari, D., Mondino, E., Mård, J., Petrucci, O., Scolobig, A., Viglione, A., and Ward, P. J.: Hess Opinions: An interdisciplinary research agenda to explore the unintended consequences of structural flood protection, Hydrol Earth Syst Sci, 22, 5629–5637, https://doi.org/10.5194/hess-22-5629-2018, 2018.

Bartiko, D., Oliveira, D. Y., Bonumá, N. B., and Chaffe, P. L. B.: Spatial and seasonal patterns of flood change across Brazil, Hydrological Sciences Journal, 64, 1071–1079, https://doi.org/10.1080/02626667.2019.1619081, 2019.

Bates, P. D. and De Roo, A. P. J.: A simple raster-based model for flood inundation simulation, J Hydrol (Amst), 236, 54–77, https://doi.org/https://doi.org/10.1016/S0022-1694(00)00278-X, 2000.

Bates, P. D., Marks, K. J., and Horritt, M. S.: Optimal use of high-resolution topographic data in flood inundation models, Hydrol Process, 17, 537–557, https://doi.org/https://doi.org/10.1002/hyp.1113, 2003.

Bhargav, A. M., Suresh, R., Tiwari, M. K., Trambadia, N. K., Chandra, R., and Nirala, S. K.: Development of a 2D hydrodynamic model for flood assessment for the lower Narmada basin, Gujarat (India), Journal of Water and Climate Change, 16, 1567–1585, https://doi.org/10.2166/wcc.2025.706, 2025.

Biancamaria, S., Lettenmaier, D. P., and Pavelsky, T. M.: The SWOT Mission and Its Capabilities for Land Hydrology, Surv Geophys, 37, 307–337, https://doi.org/10.1007/s10712-015-9346-y, 2016.

Blöschl, G.: Three hypotheses on changing river flood hazards, Hydrol Earth Syst Sci, 26, 5015–5033, https://doi.org/10.5194/hess-26-5015-2022, 2022.

Brêda, J. P. L. F., Cauduro Dias de Paiva, R., Siqueira, V. A., and Collischonn, W.: Assessing climate change impact on flood discharge in South America and the influence of its main drivers, J Hydrol (Amst), 619, 129284, https://doi.org/https://doi.org/10.1016/j.jhydrol.2023.129284, 2023.

Burrell, B. C., Davar, K., and Hughes, R.: A Review of Flood Management Considering the Impacts of Climate Change, Water Int, 32, 342–359, https://doi.org/10.1080/02508060708692215, 2007.

Cai, T., Li, X., Ding, X., Wang, J., and Zhan, J.: Flood risk assessment based on hydrodynamic model and fuzzy comprehensive evaluation with GIS technique, International Journal of Disaster Risk Reduction, 35, 101077, https://doi.org/https://doi.org/10.1016/j.ijdrr.2019.101077, 2019.

Cavalcante, M. R. G., da Cunha Luz Barcellos, P., and Cataldi, M.: Flash flood in the mountainous region of Rio de Janeiro state (Brazil) in 2011: part I—calibration watershed through hydrological SMAP model, Natural Hazards, 102, 1117–1134, https://doi.org/10.1007/s11069-020-03948-3, 2020.

Chagas, V. B. P., Chaffe, P. L. B., and Blöschl, G.: Climate and land management accelerate the Brazilian water cycle, Nat Commun, 13, 5136, https://doi.org/10.1038/s41467-022-32580-x, 2022.

Chow, V. Te: Open-channel Hydraulics, McGraw-Hill, 1959.

Collischonn, W., Ruhoff, A., Filho Cabeleira, R., Paiva, R., Fan, F., and Possa, T.: Chuva da cheia de 2024 foi mais volumosa e intensa que a da cheia de 1941 na bacia hidrográfica do Guaíba, Porto Alegre, 1–8 pp., 2024.

Collischonn, W., Fan, F. M., Possantti, I., Dornelles, F., Paiva, R., Sampaio, M., Michel, G., Magalhães Filho, F. J. C., Moraes, S. R., Marcuzzo, F. F. N., Michel, R. D. L. M., Beskow, T. L. C., Beskow, S., Fernandes, E., Laipelt, L., Ruhoff, A., Kobiyana, M., Collares, L. G., Buffon, F., Duarte, E., Lima, S., Meirelles, F. S. C., and Allasia, D.: The exceptional hydrological disaster of April-May 2024 in southern Brazil, Revista Brasileira de Recursos Hídricos, 1, https://doi.org/10.1590/2318-0331.302520240119, 2025.

Damião Mendes, M. C. and Cavalcanti, I. F. A.: The relationship between the Antarctic oscillation and blocking events over the South Pacific and Atlantic Oceans, International Journal of Climatology, 34, 529–544, https://doi.org/https://doi.org/10.1002/joc.3729, 2014.

Dawson, R. J., Ball, T., Werritty, J., Werritty, A., Hall, J. W., and Roche, N.: Assessing the effectiveness of non-structural flood management measures in the Thames Estuary under conditions of socio-economic and environmental change, Global Environmental Change, 21, 628–646, https://doi.org/https://doi.org/10.1016/j.gloenvcha.2011.01.013, 2011.

DRRS: Programa do Governo Holandês de Redução de Risco de Desastres e Suportes a Surtos (DRRS). Final Report., 2024.

Durand, M., Fu, L. L., Lettenmaier, D. P., Alsdorf, D. E., Rodriguez, E., and Esteban-Fernandez, D.: The Surface Water and Ocean Topography Mission: Observing Terrestrial Surface Water and Oceanic Submesoscale Eddies, Proceedings of the IEEE, 98, 766–779, https://doi.org/10.1109/JPROC.2010.2043031, 2010.

Dutta, D., Alam, J., Umeda, K., Hayashi, M., and Hironaka, S.: A two-dimensional hydrodynamic model for flood inundation simulation: a case study in the lower Mekong river basin, Hydrol Process, 21, 1223–1237, https://doi.org/https://doi.org/10.1002/hyp.6682, 2007.

Fernandes, E., Dyer, K. R., and Niencheski, L. F.: TELEMAC-2D calibration and validation to the hydrodynamics of the Patos Lagoon (Brazil), J Coast Res, 34, 470–488, 2001.

Fernandes, E. H. L., Dyer, K. R., Moller, O. O., and Niencheski, L. F. H.: The Patos Lagoon hydrodynamics during an El Niño event (1998), Cont Shelf Res, 22, 1699–1713, https://doi.org/https://doi.org/10.1016/S0278-4343(02)00033-X, 2002.

Fewtrell, T. J., Duncan, A., Sampson, C. C., Neal, J. C., and Bates, P. D.: Benchmarking urban flood models of varying complexity and scale using high resolution terrestrial LiDAR data, Physics and Chemistry of the Earth, Parts A/B/C, 36, 281–291, https://doi.org/https://doi.org/10.1016/j.pce.2010.12.011, 2011.

Fleischmann, A., Paiva, R., and Collischonn, W.: Can regional to continental river hydrodynamic models be locally relevant? A cross-scale comparison, J Hydrol X, 3, 100027, https://doi.org/https://doi.org/10.1016/j.hydroa.2019.100027, 2019.

François, F. S.: Modelagem hidrodinâmica de áreas suscetíveis a inundação no município de nova Santa Rita (RS), Trabalho de Conclusão de curso, Universidade Federal do Rio Grande do Sul, Porto Alegre, 2021.

Fu, L. L., Pavelsky, T., Cretaux, J. F., Morrow, R., Farrar, J. T., Vaze, P., Sengenes, P., Vinogradova-Shiffer, N., Sylvestre-Baron, A., Picot, N., and Dibarboure, G.: The Surface Water and Ocean Topography Mission: A Breakthrough in Radar Remote Sensing of the Ocean and Land Surface Water, Geophys Res Lett, 51, e2023GL107652, https://doi.org/https://doi.org/10.1029/2023GL107652, 2024.

GEBCO: GEBCO 2024 Grid, https://doi.org/doi:10.5285/1c44ce99-0a0d-5f4f-e063-7086abc0ea0f, 2024.

Ghanbarpour, M. R., Salimi, S., and Hipel, K. W.: A comparative evaluation of flood mitigation alternatives using GIS-based river hydraulics modelling and multicriteria decision analysis, J Flood Risk Manag, 6, 319–331, https://doi.org/https://doi.org/10.1111/jfr3.12017, 2013.

Gomes Calixto, K., Wendland, E. C., and Melo, D. de C. D.: Hydrologic performance assessment of regulated and alternative strategies for flood mitigation: a case study in São Paulo, Brazil, Urban Water J, 17, 481–489, https://doi.org/10.1080/1573062X.2020.1773509, 2020.

Goodess, C. M.: How is the frequency, location and severity of extreme events likely to change up to 2060?, Environ Sci Policy, 27, S4–S14, https://doi.org/https://doi.org/10.1016/j.envsci.2012.04.001, 2013.

Guse, B., Merz, B., Wietzke, L., Ullrich, S., Viglione, A., and Vorogushyn, S.: The role of flood wave superposition in the severity of large floods, Hydrol Earth Syst Sci, 24, 1633–1648, https://doi.org/10.5194/hess-24-1633-2020, 2020.

Hall, J. W., Sayers, P. B., Walkden, M. J. A., and Panzeri, M.: Impacts of climate change on coastal flood risk in England and Wales: 2030–2100, Philosophical Transactions of the Royal Society A: Mathematical, Physical and Engineering Sciences, 364, 1027–1049, https://doi.org/10.1098/rsta.2006.1752, 2006.

Hammond, J. C., Anderson, B., Simeone, C., Brunner, M., Munoz-Castro, E., Archfield, S., Magee, E., and Armitage, R.: Hydrological whiplash: Highlighting the need for better understanding and quantification of sub-seasonal hydrological extreme transitions, Hydrol Process, 39, https://doi.org/10.1002/hyp.70113, 2025.

Heinrich, P., Hagemann, S., Weisse, R., Schrum, C., Daewel, U., and Gaslikova, L.: Compound flood events: analysing the joint occurrence of extreme river discharge events and storm surges in northern and central Europe, Natural Hazards and Earth System Sciences, 23, 1967–1985, https://doi.org/10.5194/nhess-23-1967-2023, 2023.

Hendry, A., Haigh, I. D., Nicholls, R. J., Winter, H., Neal, R., Wahl, T., Joly-Laugel, A., and Darby, S. E.: Assessing the characteristics and drivers of compound flooding events around the UK coast, Hydrol Earth Syst Sci, 23, 3117–3139, https://doi.org/10.5194/hess-23-3117-2019, 2019.

Henriksen, H. J., Roberts, M. J., van der Keur, P., Harjanne, A., Egilson, D., and Alfonso, L.: Participatory early warning and monitoring systems: A Nordic framework for web-based flood risk management, International Journal of Disaster Risk Reduction, 31, 1295–1306, https://doi.org/https://doi.org/10.1016/j.ijdrr.2018.01.038, 2018.

Hillman, G., Rodriguez, A., Pagot, M., Tyrrell, D., Corral, M., Oroná, C., and Möller, O.: 2D Numerical Simulation of Mangueira Bay Hydrodynamics, J Coast Res, 2010, 108–115, https://doi.org/10.2112/1551-5036-47.sp1.108, 2007.

Hsu, S. A.: Coastal Meteorology, in: Encyclopedia of Physical Science and Technology, Elsevier, 155–173, https://doi.org/10.1016/B0-12-227410-5/00114-9, 2003.

Hunt, J. D., Silva, C. V., Fonseca, E., de Freitas, M. A. V., Brandão, R., and Wada, Y.: Role of pumped hydro storage plants for flood control, J Energy Storage, 104, 114496, https://doi.org/https://doi.org/10.1016/j.est.2024.114496, 2024.

IPCC: Climate Change 2021: The Physical Science Basis. Contribution of Working Group I to the Sixth Assessment Report of the Intergovernmental Panel on Climate Change, Cambridge University Press, Cambridge, United Kingdom and New York, NY, USA, https://doi.org/10.1017/9781009157896, 2021.

Kjerfve, B.: COMPARATIVE OCEANOGRAPHY OF COASTAL LAGOONS, in: Estuarine Variability, edited by: Wolfe, D. A., Elsevier, 63–81, https://doi.org/10.1016/B978-0-12-761890-6.50009-5, 1986.

Kundzewicz, Z. W.: Non-structural Flood Protection and Sustainability, Water Int, 27, 3–13, https://doi.org/10.1080/02508060208686972, 2002.

Laipelt, L., de Andrade, B., Collischonn, W., de Amorim Teixeira, A., Paiva, R. C. D. de, and Ruhoff, A.: ANADEM: A Digital Terrain Model for South America, Remote Sens (Basel), 16, https://doi.org/10.3390/rs16132321, 2024.

Laipelt, L., de Paiva, R. C. D., Fan, F. M., Collischonn, W., Papa, F., and Ruhoff, A.: SWOT Reveals How the 2024 Disastrous Flood in South Brazil Was Intensified by Increased Water Slope and Wind Forcing, Geophys Res Lett, 52, e2024GL111287, https://doi.org/https://doi.org/10.1029/2024GL111287, 2025.

Leonard, M., Westra, S., Phatak, A., Lambert, M., van den Hurk, B., McInnes, K., Risbey, J., Schuster, S., Jakob, D., and Stafford-Smith, M.: A compound event framework for understanding extreme impacts, WIREs Climate Change, 5, 113–128, https://doi.org/https://doi.org/10.1002/wcc.252, 2014.

Lesser, G. R., Roelvink, J. A. v, van Kester, J. A. T. M., and Stelling, G. S.: Development and validation of a three-dimensional morphological model, Coastal engineering, 51, 883–915, 2004.

Li, W., Lin, K., Zhao, T., Lan, T., Chen, X., Du, H., and Chen, H.: Risk assessment and sensitivity analysis of flash floods in ungauged basins using coupled hydrologic and hydrodynamic models, J Hydrol (Amst), 572, 108–120, https://doi.org/https://doi.org/10.1016/j.jhydrol.2019.03.002, 2019.

Lima, R. C. de A. and Barbosa, A. V. B.: Natural disasters, economic growth and spatial spillovers: Evidence from a flash flood in Brazil, Papers in Regional Science, 98, 905–925, https://doi.org/https://doi.org/10.1111/pirs.12380, 2019.

Majidi, A. N., Vojinovic, Z., Alves, A., Weesakul, S., Sanchez, A., Boogaard, F., and Kluck, J.: Planning Nature-Based Solutions for Urban Flood Reduction and Thermal Comfort Enhancement, Sustainability, 11, https://doi.org/10.3390/su11226361, 2019.

Marengo, J. A., Alcantara, E., Cunha, A. P., Seluchi, M., Nobre, C. A., Dolif, G., Goncalves, D., Assis Dias, M., Cuartas, L. A., Bender, F., Ramos, A. M., Mantovani, J. R., Alvalá, R. C., and Moraes, O. L.: Flash floods and landslides in the city of Recife, Northeast Brazil after heavy rain on May 25–28, 2022: Causes, impacts, and disaster preparedness, Weather Clim Extrem, 39, 100545, https://doi.org/https://doi.org/10.1016/j.wace.2022.100545, 2023.

Marks, K. and Bates, P.: Integration of high-resolution topographic data with floodplain flow models, Hydrol Process, 14, 2109–2122, https://doi.org/https://doi.org/10.1002/1099-1085(20000815/30)14:11/12<2109::AID-HYP58>3.0.CO;2-1, 2000.

Marques, W. C., Fernandes, E. H., Monteiro, I. O., and Möller, O. O.: Numerical modeling of the Patos Lagoon coastal plume, Brazil, Cont Shelf Res, 29, 556–571, https://doi.org/https://doi.org/10.1016/j.csr.2008.09.022, 2009.

Martins, F. and Fernandes, E.: HYDRODYNAMIC MODEL INTERCOMPARISON FOR THE PATOS LAGOON (BRAZIL), 2004.

Masood, M. and Takeuchi, K.: Assessment of flood hazard, vulnerability and risk of mid-eastern Dhaka using DEM and 1D hydrodynamic model, Natural Hazards, 61, 757–770, https://doi.org/10.1007/s11069-011-0060-x, 2012.

McMillan, H. K., Westerberg, I. K., and Krueger, T.: Hydrological data uncertainty and its implications, WIREs Water, 5, e1319, https://doi.org/https://doi.org/10.1002/wat2.1319, 2018.

Ming, X., Liang, Q., Xia, X., Li, D., and Fowler, H. J.: Real-Time Flood Forecasting Based on a High-Performance 2-D Hydrodynamic Model and Numerical Weather Predictions, Water Resour Res, 56, e2019WR025583, https://doi.org/https://doi.org/10.1029/2019WR025583, 2020.

Möller, O. O., Lorenzzentti, J. A., Stech, JoséL., and Mata, M. M.: The Patos Lagoon summertime circulation and dynamics, Cont Shelf Res, 16, 335–351, https://doi.org/10.1016/0278-4343(95)00014-R, 1996.

Neal, J., Schumann, G., Fewtrell, T., Budimir, M., Bates, P., and Mason, D.: Evaluating a new LISFLOOD-FP formulation with data from the summer 2007 floods in Tewkesbury, UK, J Flood Risk Manag, 4, 88–95, https://doi.org/https://doi.org/10.1111/j.1753-318X.2011.01093.x, 2011.

O'Loughlin, F. E., Neal, J., Schumann, G. J. P., Beighley, E., and Bates, P. D.: A LISFLOOD-FP hydraulic model of the middle reach of the Congo, J Hydrol (Amst), 580, 124203, https://doi.org/https://doi.org/10.1016/j.jhydrol.2019.124203, 2020.

Ommer, J., Neumann, J., Kalas, M., Blackburn, S., and Cloke, H. L.: Surprise floods: the role of our imagination in preparing for disasters, Natural Hazards and Earth System Sciences, 24, 2633–2646, https://doi.org/10.5194/nhess-24-2633-2024, 2024.

Paiva, R. C. D., Collischonn, W., and Buarque, D. C.: Validation of a full hydrodynamic model for large-scale hydrologic modelling in the Amazon, Hydrol Process, 27, 333–346, https://doi.org/https://doi.org/10.1002/hyp.8425, 2013.

Paiva, R. C. dias de, Mainardi Fan, F., Collischonn, W., Sampaio, M., Cristina de Oliveira, R., Lima, S., Camargo, P., and Massochin Medeiros, P.: Caracterização e modelagem das cheias de 2023 e 2024 no Rio Grande do Sul em escala regional. Relatório Técnico., 2025.

Patel, D. P., Ramirez, J. A., Srivastava, P. K., Bray, M., and Han, D.: Assessment of flood inundation mapping of Surat city by coupled 1D/2D hydrodynamic modeling: a case application of the new HEC-RAS 5, Natural Hazards, 89, 93–130, https://doi.org/10.1007/s11069-017-2956-6, 2017.

Perera, D., Agnihotri, J., Seidou, O., and Djalante, R.: Identifying societal challenges in flood early warning systems, International Journal of Disaster Risk Reduction, 51, 101794, https://doi.org/https://doi.org/10.1016/j.ijdrr.2020.101794, 2020.

Planet Team: Planet Application Program Interface: In Space for Life on Earth. San Francisco, CA , https://api.planet.com/, 2024.

Possa, T. M., Collischonn, W., Jardim, P. F., and Fan, F. M.: Hydrological-hydrodynamic simulation and analysis of the possible influence of the wind in the extraordinary flood of 1941 in Porto Alegre, RBRH, 27, e29, https://doi.org/10.1590/2318-0331.272220220028, 2022.

Poussin, J. K., Bubeck, P., Aerts, J. C. J. H., and Ward, P. J.: Potential of semi-structural and non-structural adaptation strategies to reduce future flood risk: case study for the Meuse, Natural Hazards and Earth System Sciences, 12, 3455–3471, https://doi.org/10.5194/nhess-12-3455-2012, 2012.

De Risi, R., Jalayer, F., and De Paola, F.: Meso-scale hazard zoning of potentially flood prone areas, J Hydrol (Amst), 527, 316–325, https://doi.org/https://doi.org/10.1016/j.jhydrol.2015.04.070, 2015.

Seiler, L. M. N., Fernandes, E. H. L., and Siegle, E.: Effect of wind and river discharge on water quality indicators of a coastal lagoon, Reg Stud Mar Sci, 40, 101513, https://doi.org/https://doi.org/10.1016/j.rsma.2020.101513, 2020.

Serra-Llobet, A., Jähnig, S. C., Geist, J., Kondolf, G. M., Damm, C., Scholz, M., Lund, J., Opperman, J. J., Yarnell, S. M., Pawley, A., Shader, E., Cain, J., Zingraff-Hamed, A., Grantham, T. E., Eisenstein, W., and Schmitt, R.: Restoring Rivers and Floodplains for Habitat and Flood Risk Reduction: Experiences in Multi-Benefit Floodplain Management From California and Germany, Front Environ Sci, 9, https://doi.org/10.3389/fenvs.2021.778568, 2022.

Shustikova, I., Domeneghetti, A., Neal, J. C., Bates, P., and Castellarin, A.: Comparing 2D capabilities of HEC-RAS and LISFLOOD-FP on complex topography, Hydrological Sciences Journal, 64, 1769–1782, https://doi.org/10.1080/02626667.2019.1671982, 2019.

Silva, R. A. G., Reis, R. C. S., Ramos, D. M., Belém, A. L., Puhl, E., and Manica, R.: Análise de Abertura de Novo Canal de Maré na Lagoa dos Patos para Atenuação de Cheias no Rio Guaíba, RS, in: II FLUHIDROS - Simpósio Nacional de Mecânica dos Fluidos e Hidráulica e XVI ENES - Encontro Nacional de Engenharia de Sedimentos, 2024a.

Silva, T. S., Toldo Jr., E. E., Nunes, J. C. R., Castro, N., Funke, N., Nievinski, F., Manica, R., Puhl, E., Fick, C., Scottá, F., Silva, M. L. R., and Ävila, I. M.: Nota Técnica - Vazões no Rio Guaíba durante os picos da enchente de maio de 2024, 1–2 pp., 2024b.

Silva, T. S., Toldo Jr., E. E., Nunes, J. C. R., Castro, N., Funke, N., Nievinski, F., Manica, R., Puhl, E., Fick, C., Scottá, F., Silva, M. L. R., and Ävila, I. M.: Nota Técnica - Vazões no Rio Guaíba durante os picos da enchente de maio de 2024. U, 2024c.

Stevenson, S., Coats, S., Touma, D., Cole, J., Lehner, F., Fasullo, J., and Otto-Bliesner, B.: Twenty-first century hydroclimate: A continually changing baseline, with more frequent extremes, Proceedings of the National Academy of Sciences, 119, e2108124119, https://doi.org/10.1073/pnas.2108124119, 2022.

Swain, D. L., Prein, A. F., Abatzoglou, J. T., Albano, C. M., Brunner, M., Diffenbaugh, N. S., Singh, D., Skinner, C. B., and Touma, D.: Hydroclimate volatility on a warming Earth, Nat Rev Earth Environ, 6, 35–50, https://doi.org/10.1038/s43017-024-00624-z, 2025.

Timbadiya, P. V, Patel, P. L., and Porey, P. D.: A 1D–2D Coupled Hydrodynamic Model for River Flood Prediction in a Coastal Urban Floodplain, J Hydrol Eng, 20, 05014017, https://doi.org/10.1061/(ASCE)HE.1943-5584.0001029, 2015.

USACE: HEC-RAS river analysis system hydraulic reference manual. Version 5.0, 2016.

Wang, T., Lu, Y., Liu, T., Zhang, Y., Yan, X., and Liu, Y.: The determinants affecting the intention of urban residents to prepare for flood risk in China, Natural Hazards and Earth System Sciences, 22, 2185–2199, https://doi.org/10.5194/nhess-22-2185-2022, 2022.

Wasko, C., Nathan, R., Stein, L., and O'Shea, D.: Evidence of shorter more extreme rainfalls and increased flood variability under climate change, J Hydrol (Amst), 603, 126994, https://doi.org/https://doi.org/10.1016/j.jhydrol.2021.126994, 2021.

Wulandari, S., Pratama, F., Andika, N., Wongso, P., Wijayasari, W., and Rohmat, F. I. W.: Identifying dominant river contributions to urban flooding: a scenario-based study of Makassar City, Front Built Environ, Volume 11-2025, 2025.

Zarzuelo, C., Díez-Minguito, M., Ortega-Sánchez, M., López-Ruiz, A., and Losada, M. Á.: Hydrodynamics response to planned human interventions in a highly altered embayment: The example of the Bay of Cádiz (Spain), Estuar Coast Shelf Sci, 167, 75–85, https://doi.org/https://doi.org/10.1016/j.ecss.2015.07.010, 2015.

Zhang, H., Wu, W., Hu, C., Hu, C., Li, M., Hao, X., and Liu, S.: A distributed hydrodynamic model for urban storm flood risk assessment, J Hydrol (Amst), 600, 126513, https://doi.org/https://doi.org/10.1016/j.jhydrol.2021.126513, 2021.